

Opportunities for Polymer Electrolytes in Sustaining High-Voltage Lithium Metal Batteries

Minkang Jiang, Yuhao Ma, Chuang Bao, Hao Wang, Fengrui Zhang,* Heng Zhang,* and Liping Wang*

High-voltage lithium metal batteries (HVLMBs) integrate emerging cathode materials working above 4 V (vs Li/Li⁺) with high-capacity lithium metal anode, which offer a practical solution to upgrade energy and power density of current rechargeable batteries. Replacing conventional liquid electrolytes with polymer electrolytes (PEs) further empowers HVLMBs with flexibility, processability, and enhanced safety. This is unfortunately hampered by low ionic conductivity, insufficient high-voltage stability, and poor interfacial compatibility at the anode. This review scrutinizes multifaceted strategies toward an effective implementation of PEs in HVLMBs, spanning from molecular design, material preparation, interfacial engineering, etc. Particular attention is dedicated to electrolyte preparation and the associated polymerization mechanism. Synergistic approaches harmonizing theoretical modeling, advanced material/interface engineering, and scalable manufacturing are extensively discussed. Material-level innovations to improve the mechanical integrity and flame retardancy of PE-based HVLMBs are also highlighted. The reflections and insights shared in this work are expected to smooth the barriers in combining theoretical and experimental efforts, and thus spurring the realization of practical and high-performance HVLMBs with PEs in the future energy landscape.

1. Introduction

High-voltage lithium metal batteries (HVLMBs), by virtue of ultrahigh theoretical specific capacity of lithium metal (Li⁰) anode (3860 mAh g⁻¹) and wide electrochemical potential gaps between two working electrodes, are regarded as ideal candidates for next-generation high-energy-density energy storage systems, attracting significant attention particularly for applications in electric vehicles, aerospace, and portable electronic devices.^[1–4] However, the practical realization of this technology is severely hindered by the fundamental incompatibility of conventional liquid electrolytes with both the Li⁰ anode, where they promote dendrite growth and parasitic side reactions, and high-voltage cathodes (> 4.0 V), where they undergo oxidative decomposition.^[5–7] These intrinsic limitations have compelled a strategic shift in research focus toward solid-state electrolytes to enable stable and safe HVLMBs. Among the various solid-state options, polymer electrolytes (PEs) have emerged as a particularly promising material system.^[8,9] This

is not only due to their inherent advantages such as sufficient electrochemical windows and high safety features, but also because they have lower barriers to industrialization. Compared with oxide or sulfide solid electrolyte systems, PEs are highly compatible with existing liquid-based battery production lines and benefit from a mature and low-cost raw material supply chain, making it a key and practical way to overcome the bottleneck of HVLMB today.^[10]

Although PEs exhibit distinct advantages such as low cost, simple processing, and high safety, their practical application still faces multiple challenges.^[11,12] Issues such as the low room-temperature ionic conductivity (< 10⁻⁴ S cm⁻¹) and insufficient mechanical strength of most PEs further restrict their application in high-power scenarios.^[13] In recent years, researchers have optimized PEs performance through multifaceted strategies. Beyond conventional strategies like molecular design,^[14,15] incorporation of inorganic fillers,^[16] and in situ polymerization,^[17] research is increasingly shifting toward advanced, function-oriented synthetic protocols. These emerging strategies focus on optimizing ion transport by regulating the polymer Li⁺ solvation

M. Jiang, Y. Ma, C. Bao, H. Wang, L. Wang
School of Materials and Energy
University of Electronic Science and Technology of China
Chengdu 611731, China
E-mail: lipingwang@uestc.edu.cn

F. Zhang
Tianmu Lake Institute of Advanced Energy Storage Technologies Co.
Ltd.
Liyang 213300, China
E-mail: zhangfengrui@aesit.com.cn

H. Zhang
Key Laboratory of Material Chemistry for Energy Conversion and Storage
(Ministry of Education)
School of Chemistry and Chemical Engineering
Huazhong University of Science and Technology
Wuhan 430074, China
E-mail: hengzhang2020@hust.edu.cn

 The ORCID identification number(s) for the author(s) of this article can be found under <https://doi.org/10.1002/adfm.202523096>

DOI: 10.1002/adfm.202523096

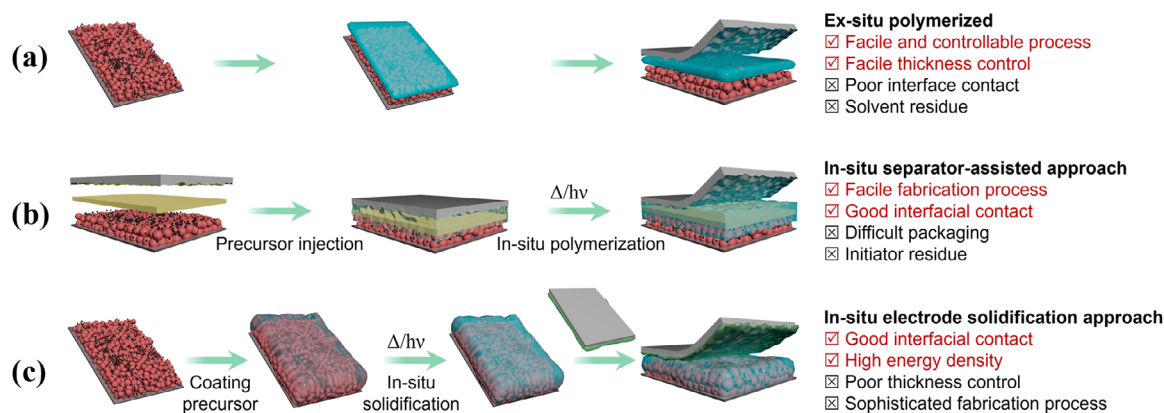


Figure 1. Various synthesized processes for polymer electrolytes in high-voltage lithium metal batteries. a) ex situ polymerization, b) in situ separator-assisted approach, and c) in situ electrode solidification approach.

environment,^[18,19] constructing specific conduction pathways using functionalized composite materials,^[20] or creating dynamic networks to impart self-healing properties to the electrolyte,^[21,22] thereby enhancing its durability and safety. In line with this trend, the sustainability of PE materials is also garnering increasing attention. Traditional PE synthesis relies heavily on petroleum-based feedstocks. To address environmental concerns and improve the circularity of battery technology, recent research efforts have begun to explore sustainable synthetic routes, including the development of PEs derived from abundant, renewable, and biodegradable materials such as cellulose, lignin, chitosan, and other biopolymers.^[23–25] These biosourced materials offer a promising green alternative, although challenges remain in optimizing their ionic transport and mechanical properties. However, their long-term cycling stability and high-voltage compatibility still urgently require improvement. Notably, while the introduction of PE systems can alleviate the safety hazards associated with liquid electrolytes, it may exacerbate electrode/electrolyte interfacial contact issues, thereby imposing more stringent requirements on their interfacial engineering.^[26]

This review delves into recent development of HVLMBs based on PEs, covering leading research achievements related to molecular design, material preparation, and interfacial engineering. First, typical preparation routes and polymerization mechanisms for PEs are discussed. Subsequently, key challenges currently encountered by PE-based HVLMBs are briefly summarized, enlisting insufficient high-voltage stability, low ionic conductivity, poor compatibility with Li^o anode, and inadequate safety performance. Multifaceted strategies for addressing these issues are then comprehensively reviewed. Finally, several prospective avenues for developing high-performance PE-based HVLMBs are outlined.

2. Overview of PE-Based HVLMBs

2.1. Preparation Methods of PE-Based HVLMBs

Common preparation methods for PEs can be categorized into ex situ and in situ techniques, based on their film-forming mechanisms.^[27–29] The core difference lies in whether the electrolyte is solidified before or after cell assembly, which critically

impacts the electrode-electrolyte interface. The most prevalent ex situ method is solution casting (**Figure 1a**), where a pre-formed PE membrane is prepared separately and then assembled with the electrodes. While this “solidify first, then assemble” process is simple, mature, and allows for effective thickness control, it inherently results in poor solid-solid interfacial contact between the electrode and the electrolyte. This leads to high interfacial impedance and potential side reactions from residual solvents, consequently degrading the cycling performance and stability of the battery.^[30,31]

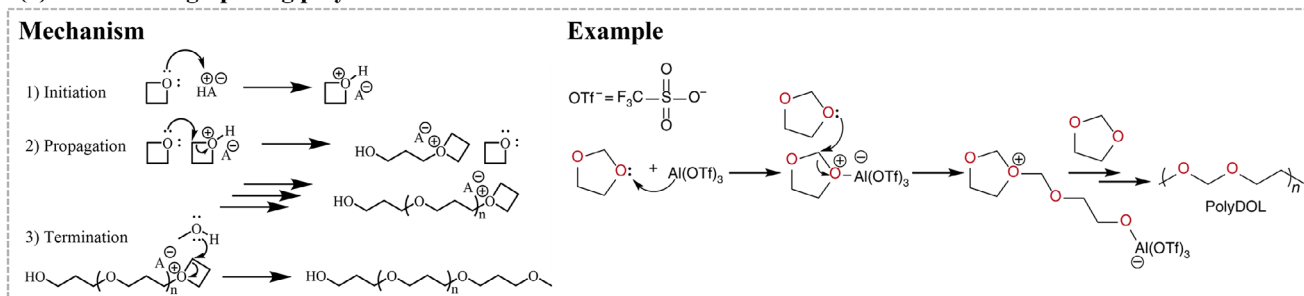
To address this critical interfacial issue, in situ polymerization methods have been developed.^[32] This strategy involves introducing a liquid precursor solution into the cell, ensuring sufficient wetting of uneven or porous electrodes before solidification (via photopolymerization or thermal polymerization).^[33–35] This “contact first, then solidify” approach facilitates intimate interfacial contact, effectively mitigating the poor contact issues prevalent in ex situ methods. In situ strategies are broadly classified into the separator-assisted approach (**Figure 1b**) and the electrode solidification approach (**Figure 1c**). The separator-assisted approach, while common, involves polymerizing the precursor within a pre-assembled cell containing a separator, but it can suffer from process challenges like glue overflow and detrimental residual initiators.^[36,37] The electrode solidification approach (**Figure 1c**) casts the precursor directly onto an electrode before assembly, offering better compatibility with high-loading cathodes. However, achieving uniform thickness over large areas is challenging, and the process is generally more complex.^[38,39]

2.2. Polymerization Mechanisms of Polymer Electrolytes

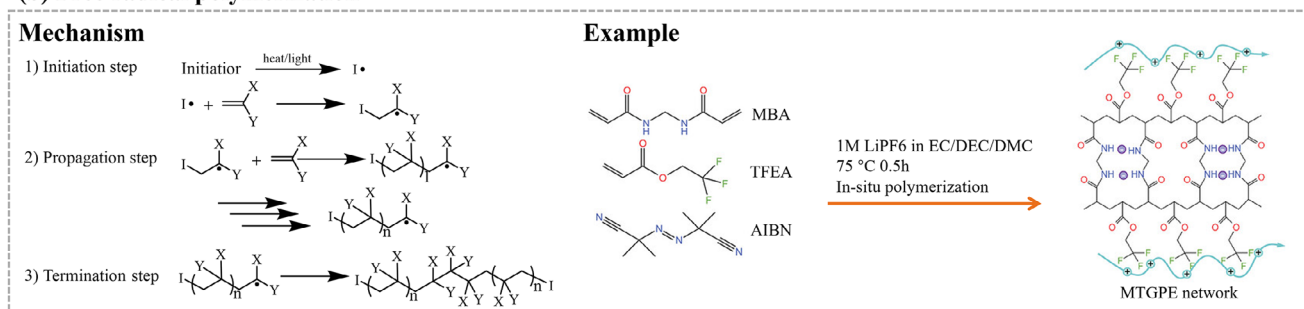
In in situ polymerization, monomers form macromolecular polymers via chemical polymerization. Common mechanisms include free radical polymerization,^[40–42] ionic polymerization,^[43,44] polycondensation reactions,^[45] and electropolymerization.^[46,47] The choice of mechanism is critical as it dictates the resulting polymer’s chain structure, molecular weight distribution, and the controllability of the process.

Cationic ring-opening polymerization (CROP), widely used for ether-based cyclic monomers, is a key example (**Figure 2a**). This

(a) Cationic ring-opening polymerization



(b) Free radical polymerization



(c) Nucleophilic addition polymerization

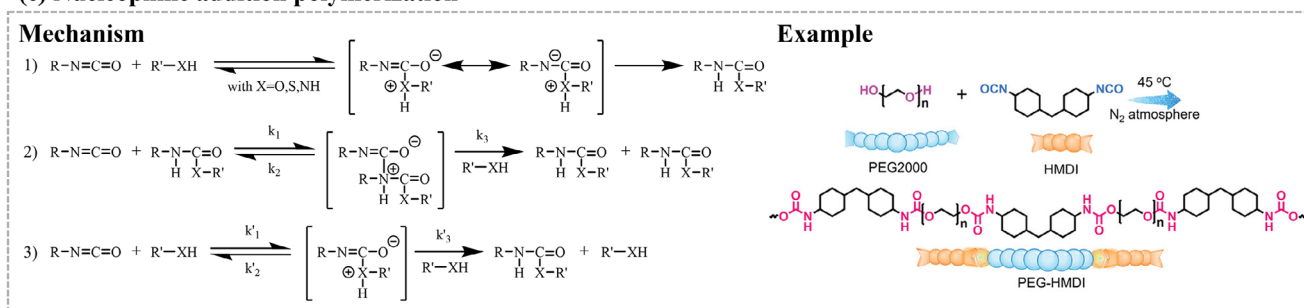


Figure 2. Key polymerization mechanisms for polymer electrolytes. a) CROP, showing the general mechanism and an example of DOL polymerization. Reproduced with permission of CC BY.^[56] Reproduced with permission.^[35] Copyright 2019, Springer Nature. b) Free-radical polymerization, detailing the mechanism and an example of network formation from MBA and TFEA. Reproduced with permission.^[57] Copyright 2015, The Royal Society of Chemistry. Reproduced with permission.^[61] Copyright 2024, Wiley-VCH. c) Nucleophilic addition polymerization, illustrating the step-growth mechanism for polyurethane synthesis. Reproduced with permission.^[59] Copyright 2012, American Chemical Society. Reproduced with permission.^[60] Copyright 2024, Wiley-VCH.

process is typically initiated by a Lewis acidic cation, such as from triflate salts^[48,49] or lithium salts^[50–54] like LiPF₆, LiBF₄ and so on, which executes a nucleophilic attack on an oxygen atom in a heterocyclic monomer. This induces repetitive ring-opening steps, propagating the polymer chain.^[55,56] The use of lithium salt initiators advantageously avoids introducing impurities. From a controllability standpoint, CROP is considered moderate. Precise molecular weight control in practical battery applications is complicated by side reactions like chain transfer, termination, and backbiting. This process generally cannot be initiated and terminated at will, offering only limited molecular weight regulation, a state known as quasi-living polymerization, by adjusting monomer-to-initiator ratios.

Another major class, free-radical addition polymerization, is used for monomers with C=C double bonds (Figure 2b). A thermal or photochemical initiator generates a free radical, which

attacks a C=C bond. This radical center propagates by attacking subsequent monomers in a process called chain propagation, until radicals combine during chain termination.^[56,57] In effect, the topological structure of the resulting polymers are highly dependent on the experimental conditions adopted therein. Conventional free-radical polymerization offers a basic ability to interrupt and resume the polymerization via temperature, but controlled/living radical polymerization (CRP) provides superior consistency. Techniques like atom transfer radical polymerization (ATRP) and reversible addition-fragmentation chain-transfer polymerization (RAFT) enable precise control over molecular weight and distribution, yielding well-defined polymer architectures. Furthermore, photo-controlled CRP, such as PET-RAFT, allows the polymerization process to be activated and deactivated externally using light, although its application in in situ battery environments remains developmental.

Other mechanisms include nucleophilic addition polymerization (Figure 2c), often used for polyurethanes. Here, a nucleophilic group, such as $-\text{OH}$ or $-\text{NH}_2$, attacks the electron-deficient carbon of an isocyanate ($\text{R}-\text{N}=\text{C}=\text{O}$), forming a carbamate or urea bond and growing the chain step-by-step.^[58–60] This mechanism offers relatively weaker process control. The degree of polymerization is highly dependent on strict stoichiometric ratios and rigorous dehydration. While it can produce polymers with a relatively narrow molecular weight distribution ($\text{PDI} < 1.5$), the reaction is not “living” and cannot be started or stopped on-demand, proceeding until monomer depletion.

2.3. Key Challenges in Developing PE-Based HVLMBs

The development of PE-based HVLMBs currently still face several hurdles such as insufficient high voltage stability, low ionic conductivity, poor compatibility with Li° anode, and relatively low inherent safety. First, the ether oxygen groups in polymers such as polyethers are prone to oxidative decomposition, triggering interfacial side reactions upon contact with high-voltage cathodes, which results in insufficient high-voltage stability. Second, due to issues like the inadequate ability of polymers to dissociate lithium salts or their tendency to crystallize, the ionic conductivity of polymer electrolytes is generally low (typically below $10^{-4} \text{ S cm}^{-1}$). Additionally, some ester-based or nitrile-based polymer electrolytes exhibit poor compatibility with lithium metal anodes. This is specifically manifested as high solid-solid interfacial impedance at the lithium metal interface, a propensity to induce lithium dendrite growth, and side reactions between the electrolyte and lithium that form an unstable solid electrolyte interphase (SEI) layer, thereby exacerbating capacity decay. Finally, compared to other inorganic solid-state electrolytes, polymer electrolytes often demonstrate insufficient safety due to their lower mechanical modulus and, for some materials, poor thermal stability. These challenges continue to hinder the development of high-performance and high-safety polymer electrolytes. In the following sections, corresponding solutions to address the aforementioned challenges will be discussed sequentially.

3. Tackling Specific Challenges in PE-Based HVLMBs

3.1. Addressing High-Voltage Stability

Strategies to enhance the high-voltage performance of PEs can be categorized into two main approaches: lowering the highest occupied molecular orbital (HOMO) of the polymer and preventing direct contact between the high-voltage cathode and the polymer. A lower HOMO level for the polymeric molecules can fundamentally improve the battery high-voltage stability. From a thermodynamic perspective, the electrolyte is resistant to oxidative decomposition when the HOMO level of each of its components is significantly lower than the operating potential of the cathode.^[62]

First, selecting polymer systems with inherently lower HOMO levels is a primary consideration. In common PE systems, polyether-based electrolytes are more susceptible to oxidation due to the presence of $-\text{C}-\text{O}-\text{C}-$ linkages, leading to poor high-voltage stability. As illustrated in Figure 3a, computational stud-

ies have shown that ester-based polymeric scaffolds, together with polyacrylonitrile (PAN), polyvinylidene fluoride (PVDF)-based PEs possess lower HOMO levels.^[62] Consequently, they exhibit superior high-voltage stability and are compatible with high-voltage cathode systems such as NCM811. Simultaneously, the oxidation of residual monomers at high voltages above 4.3 V is another factor that impacts high-voltage stability. To mitigate this, one approach is to use linear monomers, such as poly(ethylene glycol) methyl ether acrylate (PEGMA), rather than cyclic monomers (e.g., vinylene carbonate (VC), vinyl ethylene carbonate (VEC)). This can effectively increase the degree of polymerization, thereby avoiding the presence of residual monomers with high HOMO levels.^[63] Another strategy is to adopt an ex situ preparation method. In this approach, the electrolyte is assembled with the electrodes only after the monomers have been fully polymerized, which prevents the premature contact and subsequent oxidation of monomers at the high-voltage cathode, a risk inherent to in situ strategies. Furthermore, polymer molecular design strategies, including molecular fluorination, increasing steric hindrance, and chain segment extension, can also effectively lower the intrinsic HOMO level of polymer molecules.^[64] Due to the strong electronegativity of fluorine atoms, their potent electron-withdrawing capability following molecular fluorination can effectively decrease the electron density on nearby carbon atoms via the inductive effect, thereby significantly lowering the energy level of HOMO of the corresponding molecules. There are two common fluorinated monomers 2,2,2-trifluoroethyl acrylate (TFEA) and hexafluoroisopropyl acrylate (HFA), as shown in Figure 3b.^[65] Concurrently, increasing the steric hindrance of polymer molecules can also enhance their high-voltage stability. As shown in Figure 3c, the introduction of methyl groups on the poly(diethylene glycol adipate) (PDGA) backbone to increase steric hindrance can reduce its HOMO energy level from -7.98 eV (PDGA-LiTFSI) to -8.13 eV (PDMA-LiTFSI), and improve its antioxidant performance to 5.5 V. This enhancement can be attributed to the regulation of molecular orbital delocalization by methyl steric hindrance.^[49] In addition, Liu et al. found that by adding one carbon atom to the five-membered 1,3-dioxolane (DOL) to form the six-membered 1,3-dioxane (DOX), the HOMO energy level of the polymer decreased from -7.05 eV (PDOL) to -7.14 eV (P-DOX), indicating that chain extension can also improve the high-voltage stability of polymer electrolytes.^[48]

Furthermore, establishing intermolecular interactions provides another avenue to lower the HOMO of the polymer system. Intermolecular forces, such as ion-dipole interactions between lithium salts and the polymer, as well as Lewis acid-base interactions between inorganic additives and the polymer electrolyte, can alter the chemical environment of both the polymer and the lithium salt, thus modulating their HOMO levels. First, employing a high-concentration electrolyte design strategy ensures that every ether oxygen group in the polymer establishes an ion-dipole interaction with Li^+ ions. This sufficient Li^+-O coordination reduces the electron density on the ether oxygen atoms, rendering them better stability and consequently lowering the HOMO value of the corresponding polymer electrolyte.^[66] Additionally, another strategy leveraging intermolecular forces to enhance the high-voltage stability of PEs is the incorporation of inorganic fillers. As illustrated in Figure 3d, common oxide inorganic fillers such as Al_2O_3 and SiO_2 typically possess surface

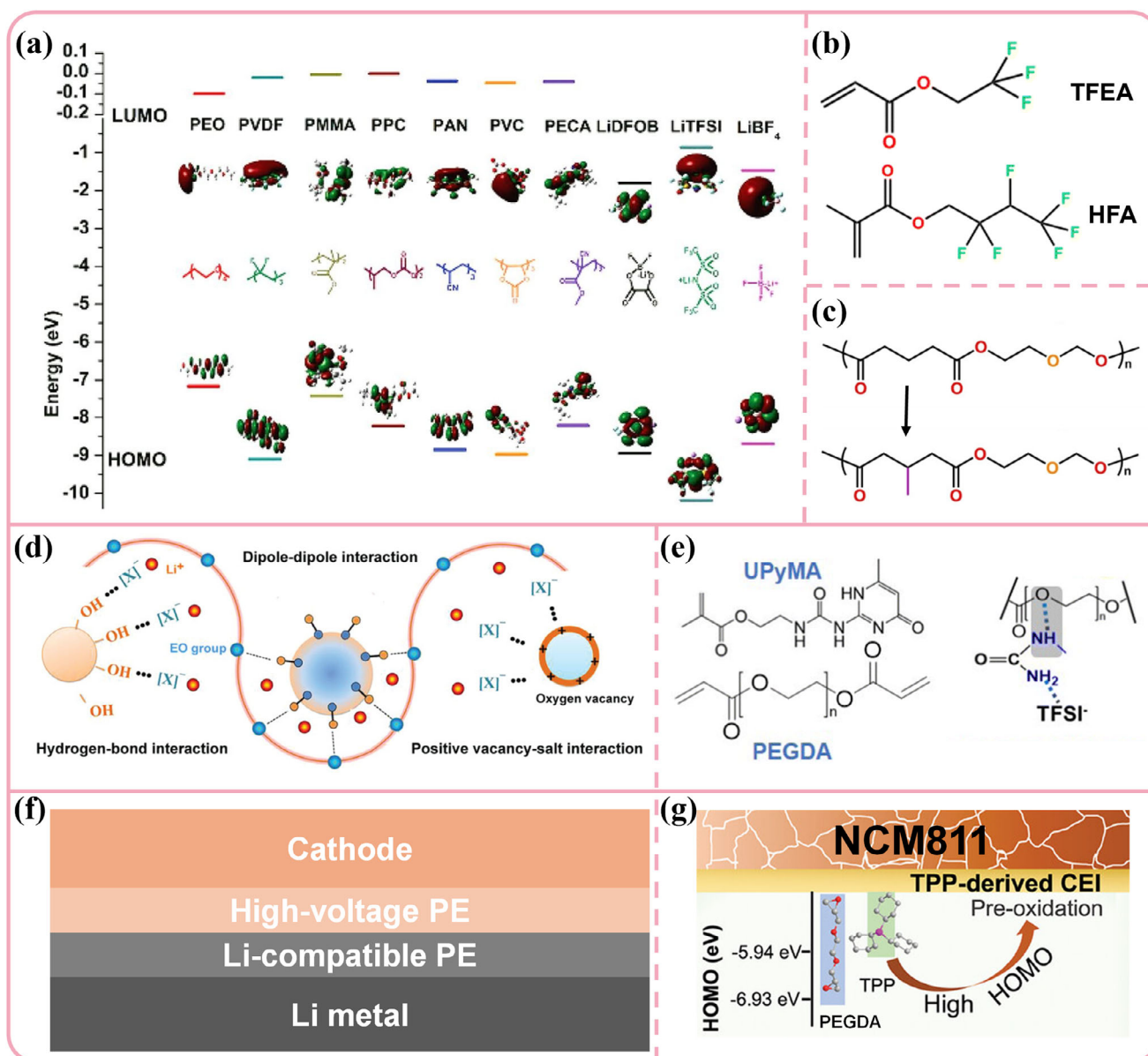


Figure 3. Improving high-voltage stability for polymer electrolyte. (a-c) Intrinsic molecular design to lower the HOMO of the corresponding polymer: a) Selecting monomers with inherently low HOMO levels. Reproduced with permission.^[62] Copyright 2019, Wiley-VCH. b) Introducing strong electron-withdrawing groups via fluorination. c) Increasing molecular steric hindrance. (d,e) Modulation of intermolecular interactions and lowering the HOMO of the entire electrolyte system: d) Inorganic fillers (Reproduced with permission.^[62] Copyright 2019, Wiley-VCH) and e) Functional additives that interact with the active oxygen species of the polymer. Reproduced with permission.^[68] Copyright 2022, The Royal Society of Chemistry. (f,g) Interfacial engineering to prevent direct contact with the high-voltage cathode: f) Constructing bilayer polymer electrolytes. g) Forming a protective CEI layer. Reproduced with permission.^[73] Copyright 2024, Wiley-VCH.

hydroxyl groups or oxygen vacancies. These Lewis acidic sites on the inorganic fillers can engage in Lewis acid-base interactions with anions: for example, through hydrogen-bond interactions, positive vacancy-salt interactions, and dipole-dipole interactions.^[62] Moreover, some inorganic fillers with a high dielectric constant, owing to their strong polarity, can establish dipole-dipole interactions with the ether oxygen groups on the polymer chains. These interactions effectively delocalize the electrons of the ether oxygens, thereby lowering the HOMO of the corresponding polymer and consequently improving its high-

voltage stability.^[67] Beyond inorganic fillers, solvent molecules within the electrolyte can also form intermolecular interactions with the polymer chains, leading to improved high-voltage performance of the battery. Wang et al.^[68] demonstrated that the amide group of *N*-methyl lactam (NML, as shown in Figure 3e) coordinates with the ether oxygen groups on poly(ethylene glycol) diacrylate (PEGDA) via hydrogen bonding, which shields the active groups on the polymer chain, thus successfully extending the electrochemical window of the corresponding PEs to 5.2 V (vs Li/Li⁺) and significantly enhancing its high-voltage stability.

Preventing direct contact between the PEs and the high-voltage cathode is also an effective strategy to improve the battery high-voltage stability. One common approach is to construct a bilayer or multilayer electrolyte, wherein a high-voltage stable electrolyte layer is formed on the cathode side (Figure 3f).^[69,70] Zhou et al.^[71] selected poly(*N*-methyl-malonic amide) (PMA) as the polymer for the high-voltage tolerant layer on the cathode side. The dimethylacetamide (DMAc)-like structural units in PMA endow it with good high-voltage stability. Concurrently, poly(ethylene oxide) (PEO) was chosen as the polymer on the anode side to ensure good anode compatibility. Another method involves building a dense cathode electrolyte interphase (CEI) film to avoid direct contact between the electrolyte and the cathode. A common strategy for CEI construction is artificial coating, with polymer coatings being a prevalent choice. Choudhury et al.^[72] coated the NCM cathode with lithiated Nafion (Lithion). The sulfonate groups in this polymer dissociate to produce negatively charged centers, forming an electrostatic shielding layer. This layer can shield the ether oxygen groups, which become negatively charged due to polarization, preventing their direct contact with the high-voltage cathode. This artificially synthesized CEI film improved the oxidative stability of ether-based electrolytes by at least 0.3 V. Furthermore, adding film-forming additives to the electrolyte for in situ CEI formation is also an effective method. Zhang et al.^[73] incorporated triphenylphosphine (TPP) into a PEGDA-based electrolyte (Figure 3g). Due to its higher HOMO (−5.94 eV), TPP is preferentially oxidized over PEGDA in the vicinity of the cathode, forming an electronically insulating CEI layer rich in Li_xPF_y and C–P bonds. This layer subsequently prevents transition metal ions from the cathode (e.g., Ni^{3+} , Co^{2+}) from contacting the electrolyte, thereby suppressing their catalytic activity toward electrolyte decomposition and extending the high-voltage stability of this ether-based electrolyte to 4.5 V.

3.2. Improving Ionic Conductivity in Bulk Electrolytes

In PE systems, Li^+ transport is generally considered to primarily depend on the concentration of lithium ions and the motion of polymer chain segments.^[74] The former is mainly related to the solvation and desolvation processes of lithium ions, while the latter is associated with the glass transition temperature (T_g) and crystallinity. Polymer chain segments in crystalline regions are immobile, with atoms only vibrating around their equilibrium positions. In amorphous regions, however, polymer chain motion is related to T_g ; a lower T_g signifies easier chain movement.

For a fixed content of lithium salt, the effective concentration of lithium ions in PEs is primarily related to the polarity of the polymer itself, which is determined by the polar functional groups within the polymer molecules. Common highly polar functional groups, as shown in Figure 4a, include ether, amino, amide, cyano, and fluorine atoms. Polymer monomers containing these functional groups can effectively promote the dissociation of lithium salts and facilitate the solvation of lithium ions.^[9,75] In addition to the selection of polymer monomers, the incorporation of inorganic fillers with Lewis acidic groups or plasticizers with strong polarity can also effectively promote lithium salt dissociation. As illustrated in Figure 4b, common inorganic fillers such as oxides like TiO_2 and SiO_2 (containing hydroxyl

groups or oxygen vacancies), and strongly polar inorganic fillers with high dielectric constants like BaTiO_3 ^[76] and SrTiO_3 ,^[77] all possess Lewis acidic sites. These sites can interact with anions from lithium salts (e.g., in LiTFSI) through Lewis acid-base interactions, thereby promoting lithium salt dissociation and increasing Li^+ concentration. Concurrently, because the anions are tethered by these Lewis acid-base interactions, the Li^+ transference number of the electrolyte can also be improved. Furthermore, Li^+ concentration is also related to the Li^+ desolvation process. Overly strong polar groups are detrimental to the decoupling of solvated lithium ions; thus, constructing a weak solvation structure is necessary. In PVDF-based polymer electrolytes, lithium ions primarily migrate as $[\text{Li}(\text{DMF})_x]^+$ complexes formed with residual *N,N*-dimethylformamide (DMF) solvent. However, the amide group in DMF is excessively polar, making it difficult for lithium ions in this solvation structure to desolvate, which is unfavorable for further Li^+ transport. To address this, some studies have employed weaker solvents with lower polarity, such as trifluoroacetic acid (TFA)^[78] or *N*-methyl trifluoroacetamide (NMTFA),^[79] to partially replace DMF. This strategy weakens the strong interaction between Li^+ and DMF, thereby establishing a weak solvation environment. Additionally, as shown in Figure 4c, DFT calculations indicate that the bond dissociation energy for $\text{C}=\text{O}-\text{Li}^+$ is $76.49 \text{ kJ mol}^{-1}$, while that for $\text{C}=\text{O}-\text{Li}$ is $116.73 \text{ kJ mol}^{-1}$. The weaker interaction strength of carbonyl-lithium complexes suggests their potential role in promoting Li^+ desolvation and enhancing Li^+ transport properties.^[80]

The T_g value dictates the extent of polymer chain segment motion and is a key determinant of the performance of polymer electrolytes, particularly at low or room temperatures. Below T_g , the polymer exists in a glassy state where chain segments are immobile, and only the constituent atoms (or groups) vibrate around their equilibrium positions.^[81] The addition of plasticizers is a highly effective method for reducing the T_g of polymer electrolytes. Common plasticizers used in polymer electrolytes include organic liquid small molecules (e.g., ethylene carbonate (EC), propylene carbonate (PC), triethylene glycol dimethyl ether (TEGD)), ionic liquids (e.g., 1-carboxymethyl-3-methylimidazole bis(trifluoromethane sulphonyl)imide ([Cmim][TFSI])^[82]), organic solid small molecules (e.g., succinonitrile (SN)), and organic macromolecules (e.g., poly(ethylene glycol) (PEG), PEGDA, poly(propylene glycol) (PPG), multi-arm boron-containing oligomer (MBO)^[83]). Figure 4d illustrates the specific mechanisms by which T_g is lowered: on the one hand, the addition of a plasticizer directly increases the space between polymer chains, thereby increasing the free volume available for polymer chain segment motion and reducing T_g . On the other hand, the added plasticizer can interact with groups on the polymer chains, replacing the original polymer-polymer intermolecular interactions. This decouples the polymer chains, also effectively lowering T_g .

Polymer crystallization is a significant challenge faced by PEO-based polymer electrolytes. In crystalline regions, polymer chain segments are unable to move, and consequently lithium ions are reluctant to migrate via polymer segmental motion. Therefore, reducing crystallinity and increasing the proportion of amorphous regions is a crucial direction for developing polymer electrolytes with high ionic conductivity. Disrupting the crystalline regions in a polymer essentially means disrupting the regular

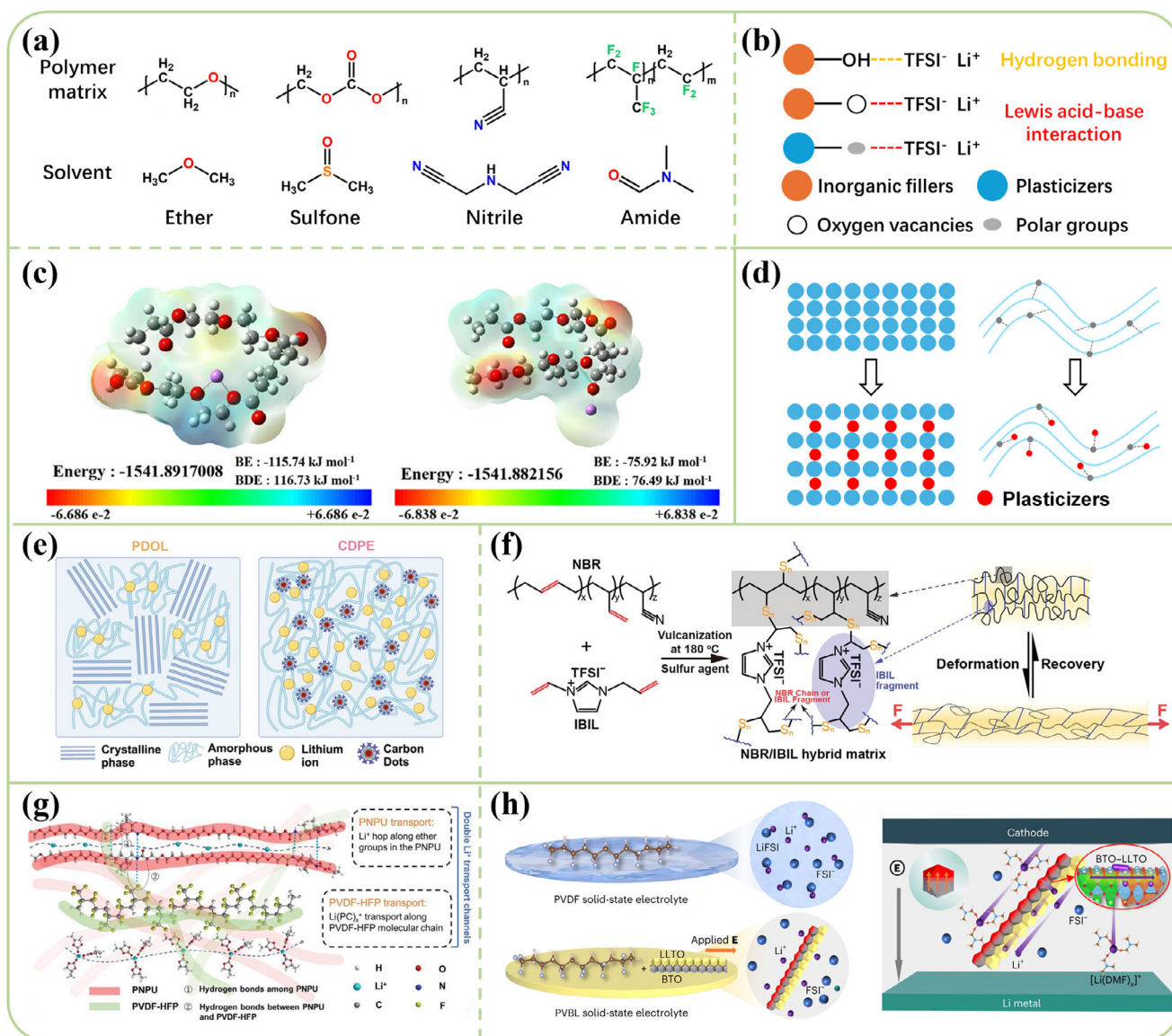


Figure 4. Improving ionic conductivity for polymer electrolyte. (a–c) Increasing free Li⁺ concentration: a) Selecting polymer molecules with strongly polar functional groups. b) Promoting lithium salt dissociation via interactions with inorganic fillers or plasticizers. c) Facilitating Li⁺ desolvation using weak solvents. Reproduced with permission.^[80] Copyright 2023, American Chemical Society. (d–f) Enhancing polymer chain segment mobility: d) Reducing T_g by adding plasticizers, e) Adding inorganic fillers to reduce crystallinity, Reproduced with permission.^[87] Copyright 2025, Wiley-VCH. f) Copolymerization to reduce crystallinity. Reproduced with permission of CC BY.^[88] (g,h) Constructing new Li⁺ transport pathways: g) Promoting directional ion migration along aligned polymer chains via intermolecular interactions like hydrogen bonding. Reproduced with permission.^[94] Copyright 2023, Wiley-VCH. h) Conduction through the bulk and surface phases of active inorganic fillers. Reproduced with permission.^[76] Copyright 2023, Springer Nature.

arrangement of polymer chain segments. The most common methods to achieve this include blending, crosslinking, and block copolymerization.^[84–86] As shown in Figure 4e, Liu et al.^[87] introduced carbon dots into P-DOL through physical blending. The abundant functional groups on the surface of the carbon dots disrupted the regular arrangement of the PDOL chains, effectively reducing the crystallinity of the polymer electrolyte. Shi et al.^[88] copolymerized an ionic-liquid-based poly(ionic liquid) (IBIL) with nitrile butadiene rubber (NBR). XRD analysis of the resulting mixed electrolyte revealed an amorphous peak around 20°, the normalized intensity of which was significantly lower

than that of the NBR electrolyte (Figure 4f). This suggested that the former possessed a higher proportion of amorphous regions and that the polymer matrix could more easily undergo local chain segment motion. In addition, Zheng et al.^[89] constructed an interpenetrating network based on PEO and poly(propylene carbonate) (PPC). After the addition of PPC, the differential scanning calorimetry (DSC) thermogram of the electrolyte showed no crystallization or melting peaks, indicating that the crystallization of PEO was suppressed.

To address the issue of low ionic conductivity, constructing new lithium-ion conduction pathways is an effective strategy.

Utilizing intermolecular interactions, such as hydrogen bonding^[90] or π - π stacking interactions^[91–93] between polymer molecules to achieve directional alignment of polymer chains, also facilitates rapid lithium-ion conduction along these chains. Ye et al.^[94] incorporated polyurethane (PNPU) into a PVDF-HFP based polymer. This introduced hydrogen bonding interactions between PNPU molecules themselves and between PNPU and PVDF-HFP (Figure 4g), leading to a side-by-side directional alignment of PNPU and PVDF-HFP. This promoted rapid, directional lithium-ion conduction along the polymer chains, and after the addition of PNPU the ionic conductivity of the polymer electrolyte increased to 4.13×10^{-4} S cm⁻¹ at 25 °C. Furthermore, among various approaches, the incorporation of active inorganic fillers is one of the most viable options. Common active inorganic fillers are categorized into garnet-type (e.g., LLZO, LLZTO), NASICON-type (e.g., LAGP, LATP), perovskite-type (e.g., LLTO), and sulfide-type (e.g., LPSCI). These active inorganic fillers inherently possess the ability to transport lithium ions, and depending on the amount added, new lithium-ion transport channels can be created.^[95] Zheng et al.^[96] experimentally demonstrated the differences in lithium ion transport paths under different LLZO addition amounts. When the LLZO concentration is only 5 wt.%, lithium ions are primarily conducted through the segmental motion of PEO chains. When the concentration reaches 20 wt.%, lithium ions predominantly rely on the interfacial pathways between LLZO and PEO for transport. At a high portion of 50 wt.% loading, lithium ions are mainly conducted through the bulk phase of LLZO, bypassing the PEO chains. Shi et al.^[76] constructed inorganic filler nanowires with a BTO-LLTO side-by-side coupled structure. In Figure 4h, BTO, with its high dielectric constant, is responsible for dissociating lithium salts and releasing lithium ions. Simultaneously, the built-in electric field of BTO can weaken the space charge layer between PVDF and the BTO-LLTO fillers, which is beneficial for lithium-ion diffusion. Subsequently, lithium ions diffuse through BTO to the LLTO side and are then conducted through the bulk and surface of LLTO. Attributed to these newly formed lithium-ion conduction pathways, the ionic conductivity of the electrolyte increased from 2.2×10^{-4} S cm⁻¹ for neat PVDF-based electrolyte to 8.2×10^{-4} S cm⁻¹ for PVBL-based one at 25 °C.

3.3. Enhancing Lithium Metal Anode Compatibility

For HVLMBs use, PE systems also face challenges regarding insufficient compatibility with Li^o anodes. On one hand, the un-suppressed growth of lithium dendrites can lead to battery short circuits. On the other hand, side reactions between the electrolyte and Li^o anode continuously consume the electrolyte, potentially leading to electrolyte depletion or gas evolution that causes cell bulging. These issues of poor anode compatibility significantly hinder the long-cycle performance of polymer electrolytes.

The formation of lithium dendrites is essentially attributed to differential lithium deposition rates caused by concentration polarization.^[97] Reducing concentration polarization can be approached from two main directions. One direction involves modifying the lithium metal anode itself, with primary strategies including the construction of 3D Li^o anodes,^[98] surface lithophilic

modification,^[99] and alloying modification.^[100] By increasing the surface area of the lithium metal and providing more nucleation sites, these methods can lower the local current density on the Li^o anode, induce uniform lithium nucleation, and thereby suppress lithium dendrite formation.^[101] The other direction is to enhance the mass transport of Li⁺, which primarily involves increasing the lithium-ion concentration and the lithium-ion transference number. Increasing Li⁺ concentration mainly depends on promoting the solvation and desolvation processes of lithium ions, as detailed in the discussion related to Figure 3. Improving the Li⁺ transference number can be achieved by immobilizing anions. Specific methods include, first, trapping anions through Lewis acid–base interactions with inorganic fillers;^[102] second, employing polyanionic polymers;^[103] and additionally, using poly(ionic liquids),^[104] which leverage the characteristic that bulky anions are less mobile, thereby increasing the lithium-ion transference number. Figure 5a shows an example where He et al.^[105] utilized polyanionic polymers to construct a polymer electrolyte that exhibited excellent lithium deposition performance. This electrolyte achieved a high Li⁺ transference number of 0.85 and a critical current density of 2.4 mA cm⁻², effectively suppressing short circuits caused by concentration polarization.

Second, utilizing the physicochemical properties of electrolytes or coatings is another approach to prevent lithium dendrites from piercing the electrolyte and causing short circuits. The most common method is to increase the mechanical modulus of the polymer electrolyte, thereby physically impeding dendrite penetration. As shown in Figure 5b, current methods to enhance mechanical modulus primarily include increasing the average molecular weight, using highly polar monomers, crosslinking, and copolymerization.^[14] Furthermore, employing anode coatings with specific characteristics, such as self-healing capabilities^[106] or high modulus,^[107] can also effectively mitigate the impact of lithium dendrites. During lithium deposition, stress can cause the SEI film to crack and rupture. The presence of a self-healing coating can promptly repair these cracks, preventing them from propagating further during repeated lithium deposition/stripping cycles.^[108] Additionally, it has been noted in existing inorganic solid-state electrolytes that lithium dendrites tend to grow along phase boundaries. Consequently, this issue might also exist at the interface between inorganic fillers and the polymer matrix in composite polymer solid electrolytes.^[109] To address this challenge in multiphase PEs, Zhang et al.^[110] prepared both phase-separated and single-phase polymer electrolytes (Figure 5c). Their research indicated that the single-phase Li-polymer in F diluter (LPIFD) exhibited a high Li deposition/stripping Coulombic efficiency (CE) of 99.1% and a critical current density (CCD) of 3.7 mA cm⁻². This superior performance was attributed to the absence of phase boundaries in the single-phase electrolyte, which promotes more uniform lithium deposition and effectively suppresses lithium dendrite formation.

Beyond the issue of lithium dendrites, side reactions between the electrolyte and lithium metal pose another significant challenge. The high reactivity of lithium metal makes it prone to react with components in the polymer electrolyte. However, not all these reactions are beneficial. In particular, ester-based polymer electrolytes severely react with lithium metal. The SEI formed from these side reactions is typically loose and porous. Such

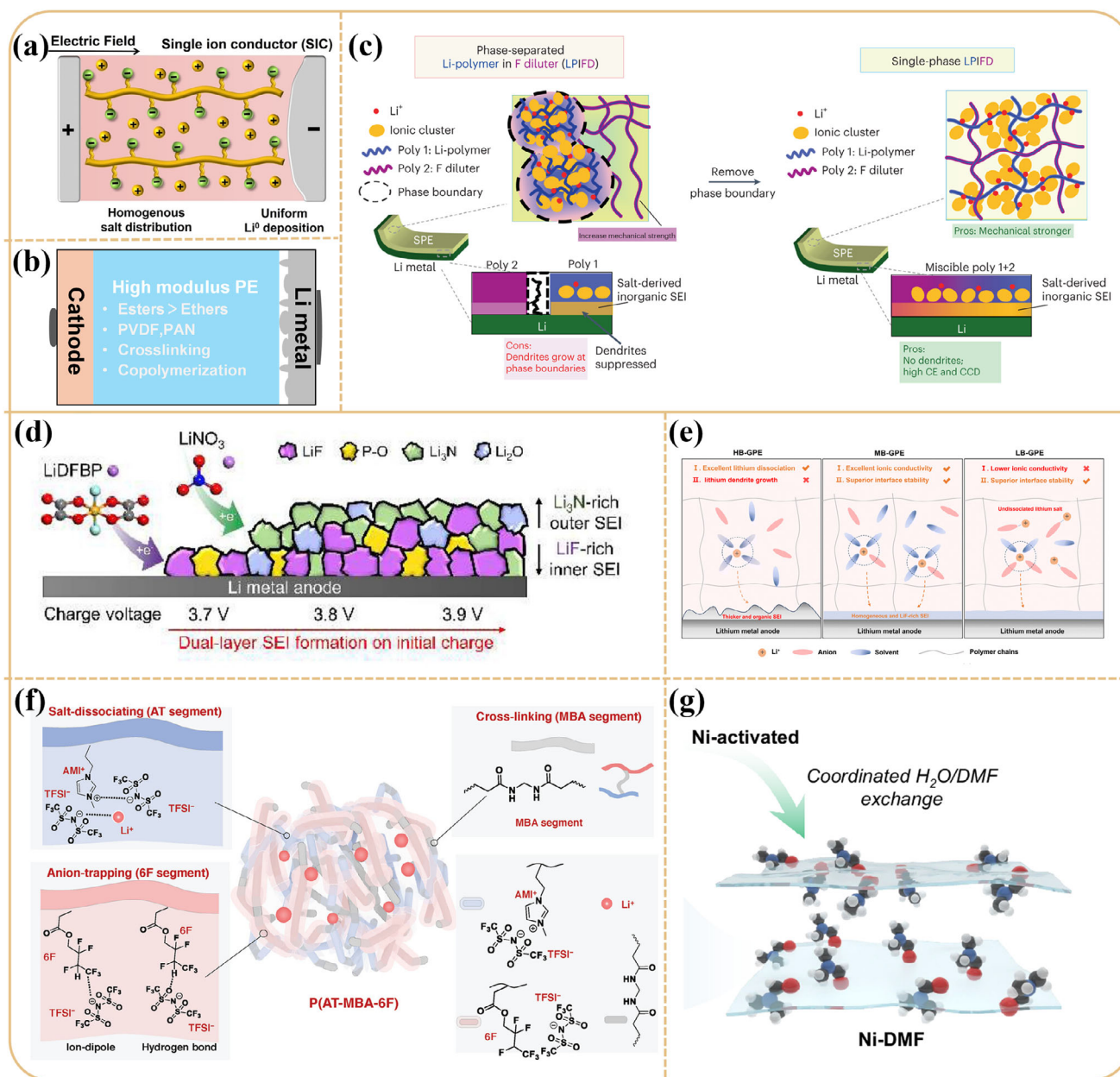


Figure 5. Improving lithium metal anode compatibility for polymer electrolyte. (a-c) Suppressing lithium dendrite growth: a) Increasing the Li^+ transference number to homogenize ion flux. Reproduced with permission.^[105] Copyright 2023, Wiley-VCH. b) Fabricating high-modulus electrolytes to physically block dendrites. c) Constructing single-phase electrolytes to ensure uniform lithium deposition. Reproduced with permission.^[110] Copyright 2024, Springer Nature. (d-g) Stabilizing the electrode-electrolyte interface: d) Building a dense, inorganic-rich SEI via film-forming additives. Reproduced with permission.^[120] Copyright 2021, Elsevier. e) Guiding SEI formation through the design of anion-rich solvation sheaths. Reproduced with permission.^[124] Copyright 2025, The Royal Society of Chemistry. f) Creating a robust, LiF-rich SEI through molecular fluorination of the polymer. Reproduced with permission.^[125] Copyright 2025, Wiley-VCH. g) Mitigating side reactions by trapping harmful residual solvent molecules. Reproduced with permission of CC BY.^[128]

a non-dense structure allows further reaction between lithium metal and the electrolyte, presenting a substantial challenge to the battery lifespan.^[111] To address such issues, the most common strategy is to isolate the lithium metal from the electrolyte. Specific approaches include forming a dense SEI film rich in inorganic components or constructing a single-ion conducting layer. As the most common film-forming method, film-forming

additives induce the formation of an inorganic SEI through preferential reduction reactions in polymer electrolyte lithium metal batteries, thereby inhibiting lithium dendrite growth and improving interfacial stability.^[112–114] Common film-forming additives include fluoroethylene carbonate (FEC),^[115] lithium difluoro (oxalate)borate (LiDFOB),^[116] lithium nitrate (LiNO_3),^[117,118] and lithium bis(fluorosulfonyl)imide (LiFSI).^[119] Figure 5d shows the

effect of two film-forming additives, LiDFOB and LiNO_3 , on the formation of a dense SEI. By introducing these two film-forming additives, Saehun et al.^[120] formed a special double-layer SEI structure with a Li_3N -rich outer layer and a LiF-rich inner layer on the negative electrode, which promoted the uniform deposition of metallic lithium. Furthermore, by constructing weak solvation structures, an anion-rich solvation sheath can be formed. This promotes the preferential reduction of anions with low lowest unoccupied molecular orbital (LUMO) energies, such as FSI^- and TFSI^- , at the anode side, leading to the formation of a LiF-rich SEI.^[121–123] In Figure 5e, non-fluorinated ethylene carbonate/ethyl methyl carbonate (EC/EMC), due to its stronger solvation capability, exhibits poor compatibility with lithium metal. In contrast, the fluorinated counterparts, FEC/FEMC and DFEC/FEMC, which exhibit weaker solvation effects, demonstrate improved compatibility with Li° anode.^[124] At the polymer level, the most common method to form a LiF-rich SEI is through molecular fluorination of the polymer. Fluorine atoms on the polymer molecule react with lithium metal to generate LiF. The fluorine atoms on the polymer molecules react with metallic lithium to generate LiF, as shown in Figure 5f. Ye et al.^[125] cross-linked the fluorine-rich monomer 2,2,3,4,4,4-hexafluorobutyl acrylate with the ionic liquid unit 1-allyl-3-methylimidazolium (AMI^+) bis(trifluoromethanesulfonyl)imide (TFSI^-) through the cross-linker MBO, in which the 6F segment with lower LUMO energy is easily reduced on Li° anode. The reaction can be initiated by the breakage of the C–F bond, releasing F-containing radicals and undergoing free radical substitution reactions with lithium compounds on the Li° anode surface. The uniform LiF-rich SEI layer can reduce the surface energy with lithium metal and promote the diffusion of Li^+ on the LiF grain boundary, which is the main reason for the formation of dendrite-free LMBs.

In polymer electrolytes, solvents often cannot be completely removed, inevitably leaving some residual solvent within the electrolyte. Furthermore, common polar solvents such as DMF or N-methylpyrrolidone (NMP) exhibit poor compatibility with metallic lithium and can undergo severe side reactions, which is detrimental to the long-term cycling of batteries. To maintain the stability of the metallic lithium interface, an effective strategy is to immobilize these residual DMF molecules, thereby inhibiting their free migration.^[126,127] Figure 5g illustrates a specific method for immobilizing DMF molecules: Zhu et al.^[128] incorporated a bifunctional layered Hofmann framework material into the electrolyte. By introducing nickel metal sites onto the Hofmann-type metal organic framework (MOF), these sites can effectively coordinate with DMF, thereby immobilizing the DMF within the Hofmann framework and enhancing the stability of the Li° anode.

3.4. Improving Inherent Safety of PE-Based HVLMBs

When compared to traditional liquid electrolytes, polymer electrolytes are typically considered safer owing to their superior mechanical strength, which enables them to effectively suppress internal short circuits (ISC) stemming from lithium dendrites. However, their safety is not fully guaranteed, particularly in the case of gel polymer electrolytes where the solvents are often

flammable, making thermal runaway a risk that cannot be entirely avoided. Figure 6a illustrates the thermal runaway process in a polymer-based lithium metal battery and the roles of its respective components. The process begins with a heat accumulation stage. Under electrical, thermal, or mechanical abuse, the SEI may decompose. Simultaneously, transition metal ions, such as Mn^{2+} , can dissolve from the cathode material and migrate to the anode side, where they further damage the SEI film. This leads to continuous reactions between the electrolyte and metallic lithium, resulting in heat accumulation. Subsequently, during the thermal runaway stage, the cathode begins to undergo lattice distortion and releases reactive oxygen. At the same time, the separator melts and collapses, while lithium dendrites grow rapidly. These events can culminate in an ISC, releasing a massive amount of heat and causing the battery temperature to rise swiftly. Finally, the combustible components within the battery, such as the polymer, undergo vigorous combustion with the released oxygen at high temperatures. This is accompanied by the generation of flammable gases like methane (CH_4), ultimately leading to an explosion.

Owing to their good flexibility, PE systems generally exhibit favorable interfacial contact properties. However, this apparent flexibility feature often leads to the disadvantage of insufficient mechanical strength, which contrasts with the characteristic of inorganic solid electrolytes that suppress lithium dendrite growth through high mechanical modulus. Therefore, enhancing the mechanical properties of polymer solid electrolytes, especially gel polymer electrolytes, is highly necessary.^[129] First, increasing the average molecular weight of the polymer can improve mechanical performance. A higher average molecular weight implies longer polymer chains and more intricate intermolecular interactions, leading to an enhancement in the polymer mechanical strength.^[130] Bao et al.^[131] investigated a series of PEO-based polymer electrolytes with different average molecular weights. As shown in Figure 6b, with increasing PEO molecular weight, the elastic modulus decreased, while the stretchability (tensile elongation) increased. The ACCE prepared from PEO ($6 \times 10^5 \text{ g mol}^{-1}$) exhibited the highest toughness ($3.87 \times 10^4 \text{ kJ m}^{-3}$) and an elongation at break of approximately 4640%. Second, the addition of inorganic fillers such as Al_2O_3 , SiO_2 , TiO_2 , and ZrO_2 can also reinforce the mechanical strength of the polymer matrix through physical crosslinking or Lewis acid-base interactions.^[132] Ma et al.^[133] incorporated SiO_2 inorganic fillers into a PVDF-based polymer electrolyte. Hydrogen bonding interactions between the surface hydroxyl groups of SiO_2 and PVDF enabled the synthesized PPSE-10 film, only 20 μm thick, to exhibit a tensile stress of 64 MPa and an elongation at break of 101.9% (Figure 6c). Furthermore, incorporating crosslinkers such as poly(ethylene glycol) diacrylate (PEGDA),^[134] tri(ethylene glycol) dimethyl ether (TEGDME),^[135] metal-organic frameworks (MOFs),^[136] or oxides^[137] to act as 3D skeletons can effectively improve the mechanical properties of the polymer. As illustrated in Figure 6d, tetraethoxysilane (TEOS) can undergo in situ hydrolysis within the polymer electrolyte to form a SiO_2 3D skeleton. This interconnected inorganic network provides structural support within the polymer, increasing the Young's modulus to a satisfactory 8.267 GPa.^[138] Finally, selecting two monomers with different mechanical strengths for copolymerization is also an effective means to improve the mechanical properties of polymer

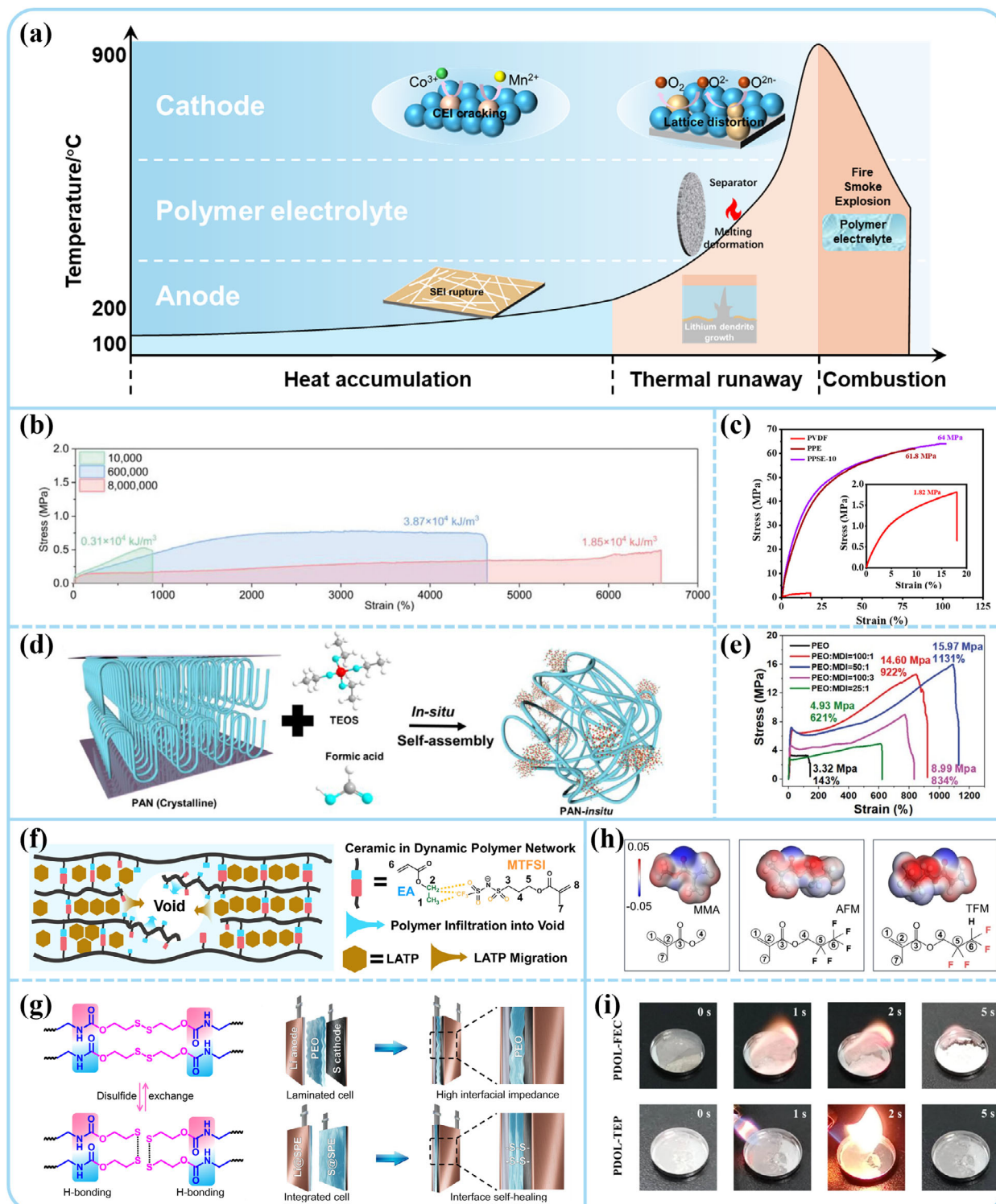


Figure 6. Improving safety for polymer electrolyte. a) Dynamic decomposition diagram of three-stage thermal runaway in Li-metal batteries. (b-e) Enhancement of mechanical properties: b) Increasing the polymer average molecular weight. Reproduced with permission.^[131] Copyright 2023, Wiley-VCH. c) Incorporating inorganic fillers for reinforcement. Reproduced with permission.^[133] Copyright 2023, American Chemical Society. d) Establishing an interconnected 3D framework. Reproduced with permission.^[138] Copyright 2021, Elsevier. e) Constructing block copolymers with hard and soft segments. Reproduced with permission of CC BY.^[140] (f, g) Construction of self-healing electrolytes, enabled by introducing dynamic reversible bonds, such as: f) non-covalent hydrogen bonds, reproduced with permission of CC BY.^[147] and g) covalent disulfide bonds. Reproduced with permission of CC BY.^[153] (h, i) Improvement of flame retardancy: h) Incorporating fluorine into the polymer structure. Reproduced with permission.^[157] Copyright 2024, Wiley-VCH. i) Adding phosphorus-containing flame retardants. Reproduced with permission of CC BY.^[158]

electrolytes.^[139] Among them, the hard segment uses a high T_g monomer such as styrene as a non-polar non-conductive component, and the soft segment uses a low T_g monomer such as PEO as a polar conductive component. Yi et al.^[140] used PEO and methylene diphenyl diisocyanate (MDI) as comonomers. PEO served as the soft segment, while MDI, with benzene rings in its main chain, constituted the rigid segment. Copolymerization resulted in an alternating arrangement of soft and hard segments. When the PEO to MDI ratio was 50:1, the tensile strength and elongation at break of the polymer increased from 3.32 MPa and 143% for pure PEO to 15.97 MPa and 1131%, respectively (Figure 6e).

Self-healing polymer electrolytes, owing to their dynamic adaptive characteristics, can effectively mitigate risks such as dendrite-induced short circuits resulting from electrolyte fracture. The self-healing property originates from reversible covalent or non-covalent interactions within the polymer molecules.^[141] Common non-covalent interactions utilized for self-healing include hydrogen bonds,^[142–144] metal–ligand coordination,^[145] and π – π stacking.^[146] Leveraging these characteristics, upon damage to the electrolyte, these supramolecular structures can reassemble to fill the damaged portions, thereby restoring the original functionality and integrity. He et al.^[147] constructed a dynamically crosslinked aprotic polymer based on non-covalent $-\text{CH}_3\cdots\text{CF}_3$ hydrogen bonds. The reversible breaking and reformation of these hydrogen bonds enable the adaptive migration of ceramic particles within the polymer matrix. This facilitates a two-step self-healing mechanism: initially, the polymer electrolyte infiltrates any voids, followed by the migration of micro-sized LATP particles through the polymer electrolyte matrix to fill these voids (Figure 6f). Reversible covalent bonds employed in polymer electrolytes include disulfide bonds,^[148] boron-based bonds,^[149,150] Diels–Alder chemistry,^[151] and imine bonds.^[152] These covalent bonds are generally stronger than non-covalent bonds, effectively enhancing the mechanical properties of the polymer electrolyte while also providing excellent self-healing capabilities. As shown in Figure 6g, Pei et al.^[153] introduced 2-hydroxyethyl disulfide (BHDS) to form dynamic covalent disulfide bonds, thereby constructing a self-healing polyether-urethane based electrolyte. This approach successfully overcame the common issues of multiple interfacial contacts often encountered in solid-state electrolytes.

In addition to mechanical strength, which primarily prevents internal short circuits, flame retardancy is a critical aspect of overall PE safety, as the predominantly organic components can serve as fuel in a thermal runaway event. The currently common method involves adding phosphorus- or fluorine-containing flame retardants.^[154] These retardants function by releasing F radicals or phosphate-oxy radicals upon pyrolysis, which then scavenge the active hydrogen and oxygen radicals generated from the thermal decomposition of the electrolyte or cathode, thereby achieving flame retardancy.^[155,156] Figure 6h shows poly(2,2,3,3-tetrafluoropropyl methacrylate) (PTFM), synthesized by introducing fluorine-containing electron-withdrawing groups onto poly(methyl methacrylate) (PMMA). Combustion tests demonstrated its good flame retardancy. This is attributed to the fluorine elements in the electron-withdrawing groups of the polyester, which can capture oxygen radicals during the combustion of the organic electrolyte, thereby suppressing the burning of the CP-GPE.^[157] In Figure 6i, Tang et al.^[158] introduced triethyl phos-

phate (TEP) as a flame retardant into a PDOL-based system, resulting in a flame-retardant and safe gel polymer electrolyte, PDOL-TEP.

4. Full-Cell Performance and Safety Testing of PE-Based HVLMBs

The preceding sections have detailed the multifaceted strategies employed to address the individual challenges of high-voltage stability, ionic conductivity, anode compatibility, and inherent safety. However, the ultimate measure of success for any polymer electrolyte is not the optimization of a single parameter, but its ability to function effectively as part of an integrated, high-performance full cell. Therefore, this chapter shifts the focus from material-level strategies to the state-of-the-art performance demonstrated in complete PE-based HVLMBs, critically examining the current benchmarks and the practical challenges of achieving a holistic balance of energy density, cycle life, and safety.

Table 1 summarizes a selection of state-of-the-art, high-voltage polymer electrolyte full cells reported recently, providing a benchmark for the discussion in this section. From a performance perspective, recent breakthroughs have redefined the benchmarks for polymer-based batteries. In terms of energy density, by coordinating PEO with strong Lewis acids such as Mg^{2+} and Al^{3+} , systems compatible with high-voltage cathodes (4.8 V) have achieved remarkable pouch cell energy densities reaching as high as 586 Wh kg^{-1} .^[159] Regarding long-term cycling stability, the design of an *N*-methyl-2,2,2-trifluoroacetamide (NMTFA) ligand, which lowers the Li^+ desolvation energy and activates interfacial Li^+ exchange, has enabled a PVDF-based composite polymer electrolyte to achieve stable cycling for over 10 000 cycles at a high rate of 10C.^[78] The most significant advantage of polymer electrolytes, however, emerges when considering safety. While delivering competitive energy densities, polymer electrolyte batteries exhibit intrinsically superior safety profiles. This advantage is particularly critical for high-energy systems employing high-nickel cathodes (e.g., NCM811), which are notoriously prone to thermal runaway when paired with liquid electrolytes. In stark contrast, many high-performance pouch and cylindrical cells based on polymer electrolytes have been shown to successfully pass stringent industry-standard safety evaluations, such as nail penetration tests^[160] and accelerating rate calorimetry (ARC) tests,^[161] without fire or explosion. This represents a critical safety milestone that remains a significant challenge for their liquid-based counterparts operating at similar high-energy levels.

To assess the practical viability of polymer electrolytes, however, their performance must be evaluated in full-cell configurations under conditions relevant to commercial applications. This typically involves using high-areal-capacity cathodes and anodes ($> 4 \text{ mAh cm}^{-2}$), a restricted negative-to-positive capacity (N/P) ratio (approaching 1.0), and a lean electrolyte content (e.g., $< 2 \text{ g Ah}^{-1}$). While this high-energy configuration is essential for maximizing gravimetric and volumetric energy density, it places immense stress on the electrolyte and its interfaces. Consequently, a critical trade-off often emerges: cells optimized for the highest energy density frequently exhibit poor cycling stability. The limited amount of electrolyte and the small excess of lithium metal cannot accommodate significant parasitic reactions, leading to rapid capacity fade.

Table 1. Recent progress in pouch cells of PE-based HVLMBs.

Polymer/salt/others	Ionic conductivity [mS cm ⁻¹]	Thickness	Preparation method	Full cell	Capacity of pouch cells	Energy density [Wh Kg ⁻¹]	Capacity retention	Nail penetration test	Refs.
PEG-HMDI+ZrMOF/LITFSI	0.57 at 30 °C	≈20 μm	In situ	Li NCM811	≈1.5 Ah	400	> 75 cycles	✓	[60]
PEO/LITFSI/AI(C10)3+Mg(ClO ₄)2	0.23 at 25 °C	<40 μm	Ex situ	Li NCM83	✓	586	63.5% at 100 cycles	✓	[159]
PVDF/LiFSI/DMF+TTE	1.27 at 25 °C	✓	Ex situ	Li NCM811	✓	354.4	78.1% at 450 cycles	Pass	[165]
BEPEB/UDFOB+UBF4+UTFSI/FEC+FEMC+UDFP	1 at 25 °C	25 μm	In situ	Li NCM811	5.6 Ah	405.3	87.2% at 15 cycles	Pass	[166]
DOL+CTA/LITFSI+LiDFOB/Zn (TFSI) ₂ +FEC+DEC	1.01 at 20 °C	≈16 μm	In situ	Li LCO	18 Ah	452	95.2% at 100 cycles	Pass	[167]
FMA+FEP+PEGDA/LITFSI/FEC	0.44 at 25 °C	≈25 μm	In situ	Li NCM811	5.4 Ah	451	✓	✓	[168]
DVTU+PETEA/UPF6/EC+DEC	1.31 at 25 °C	✓	In situ	Li NCM811	6 Ah	485	> 12 cycles	✓	[169]
PETA/LiPF6/EC+DEC	✓	✓	In situ	Li NCM811	4.5 Ah	455	80.7% at 210 cycles	✓	[170]
PETEA+PFBA/LiPF6/EC+DEC	0.56 at 20 °C	✓	In situ	Li NCM811	4.4 Ah	381	83.4% at 120 cycles	Pass	[171]
ATU+HEAC+PETE/UPF ₆ /DMC+EC+EMC+FEC	3.09 at 25 °C	31 μm	In situ	Li NCM811	6.46 Ah	412	99% at 20 cycles	Pass	[172]
TFPO+PEE/LiDFOB+UTFSI/FEC+DMC	3.98 at 25 °C	25 μm	In situ	Li NCM622	0.2 Ah	✓	81.4% at 60 cycles	Pass	[173]
DOL+OFHDBO/UDFOB+LiTFSI/FEC+DMC	1.47 at 25 °C	✓	In situ	Li NCM811	1.1 Ah	401.8	> 16 cycles	Pass	[174]
MMA+MMAm/LiFSI/SN+FEC	2.8 at 25 °C	≈20 μm	In situ	Li NCM811	5 Ah	456	95% at 40 cycles	Pass	[175]

The evaluation of battery safety is conducted through a combination of material-level and cell-level testing. At the material level, thermal analysis techniques such as ARC and differential scanning calorimetry (DSC) are used to determine the onset temperature of exothermic reactions between the electrolyte and the electrodes.^[162–164] At the cell level, mechanical abuse tests like nail penetration, crush, and overcharge tests are critical for simulating real-world failure scenarios. However, there are notable limitations with these current evaluation methods. First, safety performance is highly scale-dependent; a small lab-scale pouch cell that passes a nail penetration test does not guarantee that a large-format commercial cell with different thermal management properties will behave similarly. Second, the industry still largely relies on safety standards originally developed for liquid electrolytes, which may not be fully adequate for capturing the unique degradation-to-failure pathways of solid-state systems. Finally, current abuse tests primarily focus on the response to a catastrophic internal short circuit and may not sufficiently assess other critical safety issues relevant to polymer electrolytes, such as gas generation from slow electrolyte decomposition.

While Table 1 highlights impressive achievements in individual metrics, systems that achieve a comprehensive balance of all key metrics are particularly instructive for future design. A recent milestone in the development of practical polymer electrolyte batteries is exemplified by the work of Wang et al.^[175] on a gel polymer electrolyte (GPE), which demonstrates a comprehensive solution for balancing the competing demands of energy density, cycle life, and safety in commercially relevant pouch cells, as illustrated in Figure 7. The success of this system is rooted in the “competitive ion coordination” strategy of the PMAm-SN electrolyte, a concept depicted in Figure 7a. This unique design decouples mechanical strength from ionic conductivity by using a highly polar solvent (e.g., succinonitrile) to coordinate with Li⁺ ions, which preserves the polymer own hydrogen-bonding network. This results in both a mechanically robust electrolyte and the formation of a highly stable, inorganic-rich SEI.

This superior material design directly translates to outstanding full-cell performance. The stable interface enables excellent cycling longevity, as demonstrated by the 1 Ah pouch cell which maintains approximately 90% of its initial capacity over 100 cycles (Figure 7c). The electrolyte high performance also allows for the fabrication of practical, high-capacity cells where the weight of active materials is maximized (Figure 7b). This is showcased by a 5 Ah pouch cell that achieves a remarkable, pack-level (including packaging) energy density of 456 Wh kg⁻¹ (Figure 7d), a value that significantly exceeds the 400 Wh kg⁻¹ threshold for next-generation batteries.

Crucially, this high energy density is achieved without compromising safety. The pouch cells exhibit exceptional thermal stability, with a high onset temperature for thermal runaway of 135 °C in ARC tests (Figure 7e). Furthermore, they show remarkable resilience to mechanical abuse, with the cell temperature rising to only 37 °C during stringent nail penetration tests (Figure 7f). This powerful combination of high energy density, stable cycling, and proven safety in a practical pouch cell format demonstrates its potential to meet the stringent requirements of emerging applications. For instance, the ability of the 1 Ah pouch cell to power a drone in a test flight, as shown in Figure 7g,

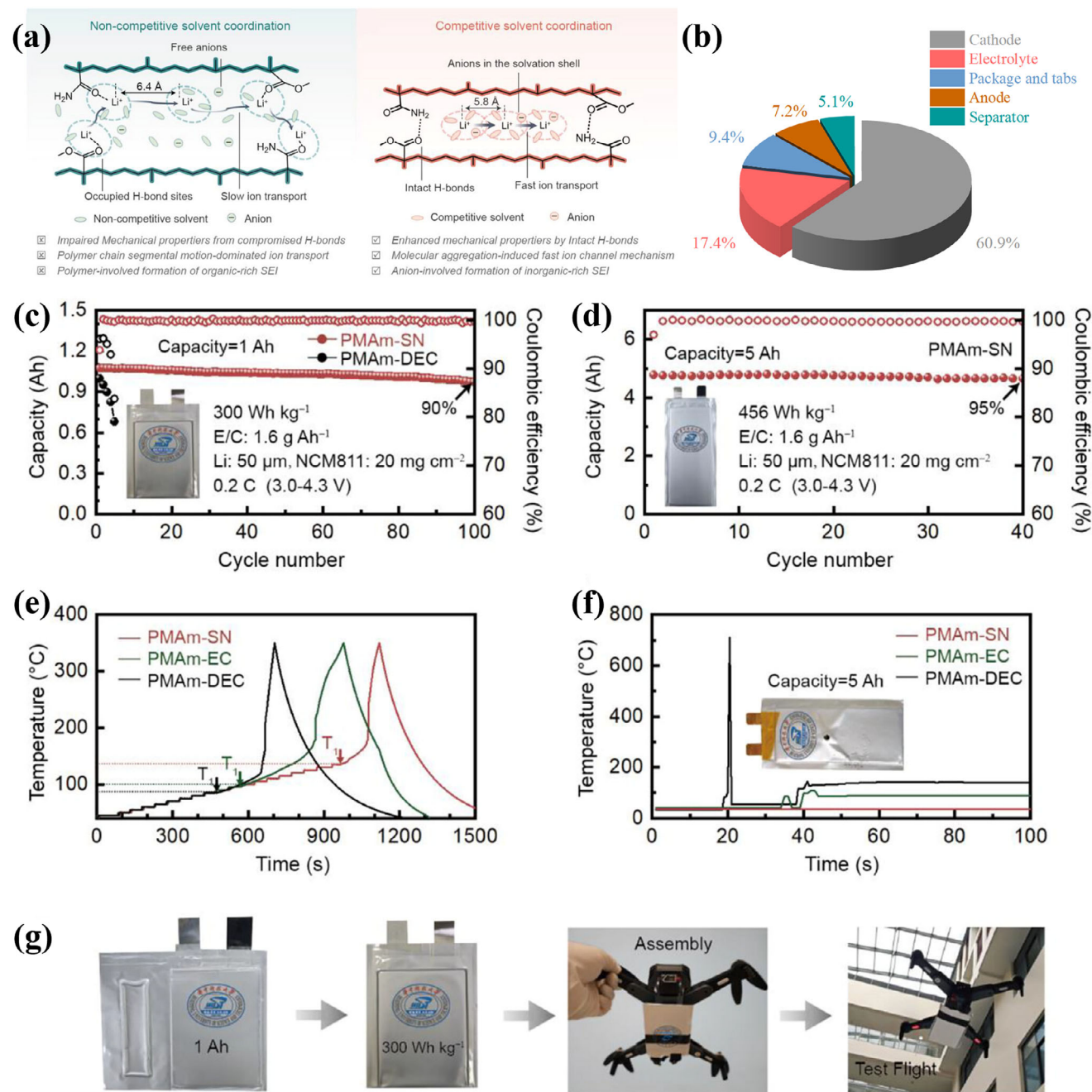


Figure 7. Electrochemical stability and safety performance of Li/PMAm-SN GPEs/NCM811 pouch cells. a) PMAm-SN GPEs design strategy. b) Proportion of each component in a 5 Ah PMAm-SN GPEs soft pack battery. c, d) Cyclic performance of Li/PMAm-SN/NCM811 pouch cell with 1 Ah (c) and 5 Ah (d) capacities. e) ARC results of fully charge Li/NCM811 cells with different electrolytes. f) Temperature evolution during nail penetration tests. g) Drone powered by a 1 Ah pouch cell using PMAm-SN. Reproduced with permission.^[175] Copyright 2025, Wiley-VCH.

highlights its suitability for the demanding, safety-critical low-altitude economy. This work therefore provides a compelling demonstration that well-engineered polymer electrolytes can enable the fabrication of large-format pouch cells that successfully unify high energy density, stable cycling, and a high degree of safety.

5. Opportunities for PE-Based HVLMBs

On the basis of the above status-quo analyses and our experiences in this domain, the following key directions and opportunities for building more attractive PE-based HVLMBs are recommended (Figure 8).

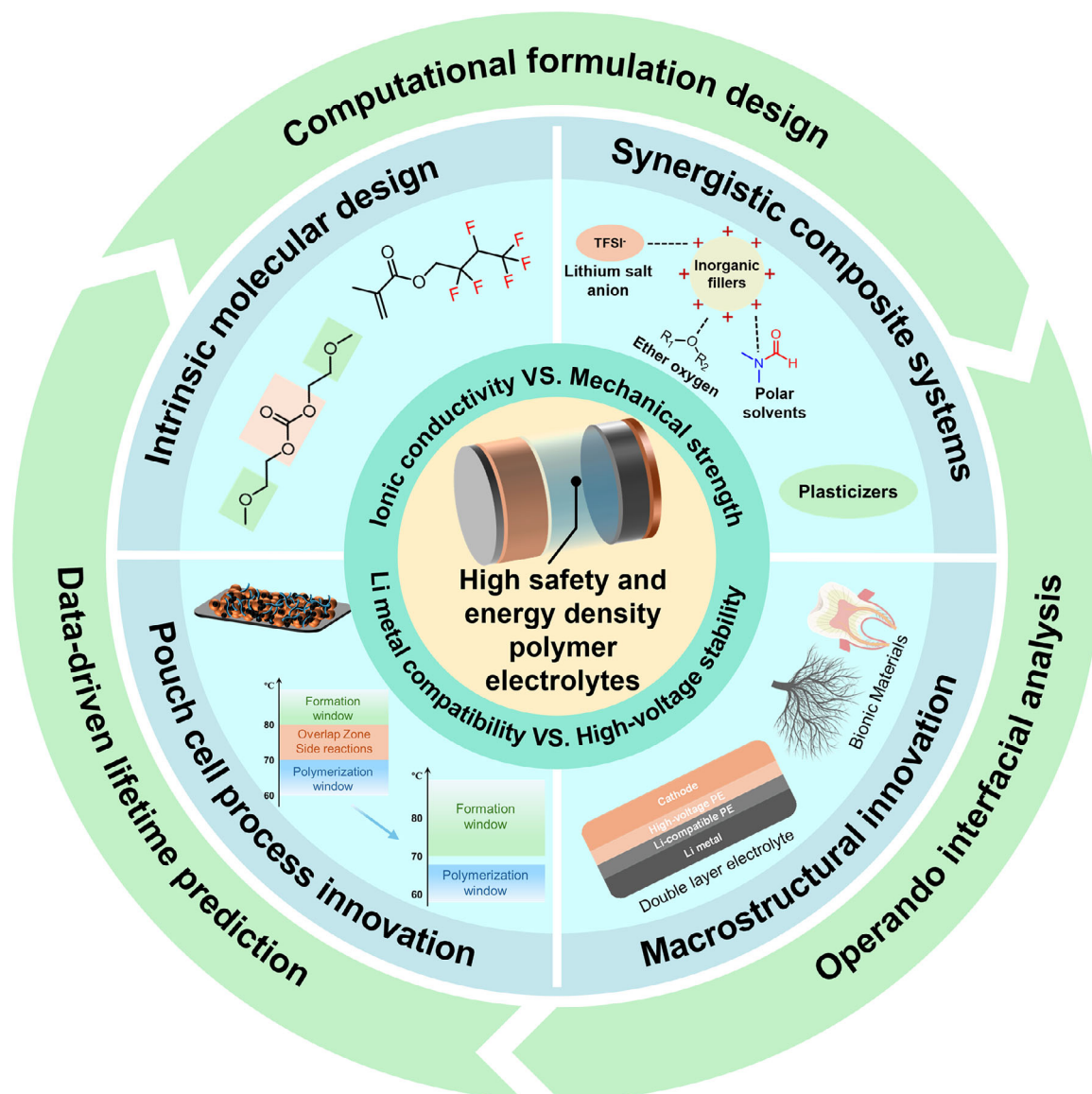


Figure 8. Future perspectives and key research thrusts for high safety and energy density polymer electrolytes.

- 1) Intrinsic optimization and multifunctionality of polymer and metal salts' molecular structures are fundamental. This requires researchers to develop novel polymer backbones and salt anions through elegant molecular design. The goal is to create macromolecular architectures where a wide electrochemical stability window, high ionic conductivity, a high lithium-ion transference number ($T_{Li^+} > 0.5$), and robust mechanical strength are synergistically integrated, not merely balanced. A more unique insight is to design polymers that actively manage the Li^+ solvation sheath, for instance, by featuring functional groups that selectively coordinate with anions, to intrinsically boost the Li^+ transference number while minimizing interfacial impedance.
- 2) Building upon optimized polymer matrices, the development of synergistically enhanced composite PE systems is a key strategy for improving overall performance. By judiciously in-

corporating inorganic fillers with specific functions (e.g., fast ion-conducting ceramics, high-dielectric-constant nanoparticles), ionic liquids, or other functional polymers into the host polymer matrix, specific performance aspects can be targeted for improvement. A deeper perspective involves moving beyond simple blending to focus on the rational design of the polymer-filler "interphase", a distinct third phase the controlled structure and chemistry of which can be engineered to create preferential ion conduction pathways while enhancing mechanical cohesion.

- 3) Macrostructural innovation in electrolyte systems offers new dimensions for resolving complex trade-offs. The development of asymmetric polymer electrolytes allows for the separate optimization of the anode and cathode interfaces by stacking different functional layers, thereby decoupling competing performance metrics. Concurrently, developing

ultrathin polymer electrolytes is crucial for increasing the active material ratio and lowering overall cell impedance, enabling pouch cells with energy densities exceeding 400 Wh kg⁻¹. Furthermore, bio-inspired and biomimetic strategies offer a paradigm-shifting avenue. By mimicking the unparalleled ion selectivity and transport efficiency of biological ion channels, future research could design polymer electrolytes with ordered, sub-nanometer channels that decouple ion transport from polymer segmental motion, potentially solving the conductivity-strength dilemma.

- 4) The transition from laboratory-scale coin cells to commercially viable pouch cells imposes significantly more stringent requirements. A primary challenge is ensuring thorough electrolyte penetration into high-loading cathodes, which can be addressed by refining in situ polymerization processes or engineering the cathode's porosity. Another critical hurdle is thermal management during in situ polymerization, where heat can trigger premature cell formation processes. Precisely controlling the thermal profile to decouple the polymerization and formation windows is therefore paramount. Looking toward industrial-scale production, a forward-looking consideration is the development of in-line, non-destructive quality control techniques, such as ultrasonic mapping or magnetic field imaging, to monitor polymerization uniformity and interface quality during manufacturing, ensuring the high cell-to-cell consistency essential for commercial battery packs.^[176,177]
- 5) The synergy of advanced computation, data science, and characterization must evolve from a supportive role to the central engine of discovery, accelerating the transition from "trial-and-error" to "rational design". A pragmatic yet forward-looking approach should focus on the following concrete directions. First, computational efforts should prioritize building "digital libraries" of high-value chemical components by using methods like molecular dynamics (MD) simulations, the accuracy and scale of which can be vastly improved with machine learning force fields (MLFFs).^[178] This allows machine learning models, particularly graph neural networks (GNNs), to perform rapid "in-silico formulation screening" by mixing and matching these pre-vetted components to predict the properties of complex electrolytes. Second, this computational work must be closely coupled with advanced characterization aimed at solving the critical challenge of the buried solid-solid interface. The development and application of interface-sensitive operando techniques, such as sum-frequency generation (SFG) spectroscopy or correlative methods like combined in situ Raman and in situ EIS,^[179,180] is crucial for quantitatively understanding the chemical and morphological evolution of the SEI in real-time. Finally, the most immediate and practical impact of data science will be to develop predictive models for long-term cycling stability based on short-term electrochemical data. By training machine learning models, from powerful gradient boosting algorithms like XGBoost on engineered features to deep learning architectures like RNN and LSTM on raw time-series data, to recognize degradation "fingerprints" in the dQ/dV curves and impedance spectra of the first few dozen cycles, we can drastically reduce development time.^[181,182] This integrated, problem-focused workflow represents the most effective path

toward the rational engineering of next-generation polymer electrolytes.

- 6) Finally, as high-voltage lithium metal batteries advance toward commercial use in electric vehicles and safety-critical applications like the low-altitude economy, safety must be treated as the most crucial, non-negotiable performance metric. While polymer electrolytes offer an intrinsically safer platform compared to their liquid counterparts, as demonstrated by their ability to pass abuse tests where conventional cells fail catastrophically, the research community must adopt more rigorous and standardized validation protocols to ensure laboratory promise translates to real-world reliability. Therefore, we propose two essential considerations for future safety evaluations. First, true safety validation must move beyond small-scale coin cells. We strongly advocate that abuse tests, such as nail penetration, be conducted on commercially relevant, Ah-level pouch cells. This is critical because failure mechanisms and thermal management are highly scale-dependent, and performance in small cells does not guarantee safety in larger formats. Second, a comprehensive safety assessment must include fundamental thermal analysis. Thermal abuse tests like ARC and DSC are indispensable, as they provide quantitative, intuitive data on the onset temperature of exothermic reactions and the total heat generated during the thermal runaway process. This information is vital for designing safer materials and effective pack-level thermal management systems. By establishing and adhering to these more rigorous and multi-scale safety validation standards, the field can build the necessary confidence for the widespread adoption of polymer electrolyte-based batteries in the most safety-critical applications of the future.

6. Conclusion

By virtue of their exceptional energy density potential, HVLMs are regarded as a core development direction for next-generation energy storage technologies. PEs have garnered widespread attention in this field owing to their inherent flexibility, ease of processing, and significant potential for enhancing intrinsic battery safety. Although existing research has achieved breakthroughs in full-cell performance, practical application is impeded by a classic materials science challenge: resolving the inherent trade-offs between key electrolyte functionalities. High ionic conductivity is often achieved at the expense of mechanical strength, while high-modulus electrolytes face increased interfacial impedance. Therefore, future research activities focusing on strategies that balance "rigidity and flexibility" are of utmost importance. Concurrently, the insufficient cycling stability of high-energy-density systems necessitates the development of effective antioxidative additives, and the viability of scalable manufacturing processes remains a critical hurdle for industrial feasibility. Comprehensively, optimizing full-cell performance requires a synergistic, multidimensional approach encompassing molecular design, interface engineering, and process innovation to ultimately unify high specific energy, long cycle life, and intrinsic safety. With all these efforts implemented, the PE-based HVLMs are anticipated to stand out among electrochemical energy storage techniques for sustaining future energy network.

Acknowledgements

This work was supported by the National Natural Science Foundation of China (Nos. 22322903 and 22579023), the Natural Science Foundation of Sichuan, China (No. 2023NSFSC1914), and Beijing National Laboratory for Condensed Matter Physics (2023BNLCMPKF015).

Conflict of Interest

The authors declare no conflict of interest.

Keywords

high energy density, high safety, polymer electrolyte, solid-state lithium battery

Received: September 1, 2025

Revised: November 3, 2025

Published online:

- [1] M. Armand, J. M. Tarascon, *Nature* **2008**, 451, 652.
- [2] J. Liu, Z. Bao, Y. Cui, E. J. Dufek, J. B. Goodenough, P. Khalifah, Q. Li, B. Y. Liaw, P. Liu, A. Manthiram, Y. S. Meng, V. R. Subramanian, M. F. Toney, V. V. Viswanathan, M. S. Whittingham, J. Xiao, W. Xu, J. Yang, X.-Q. Yang, J.-G. Zhang, *Nat. Energy* **2019**, 4, 180.
- [3] L. Wang, Z. Wu, J. Zou, P. Gao, X. Niu, H. Li, L. Chen, *Joule* **2019**, 3, 2086.
- [4] J. W. Choi, D. Aurbach, *Nat. Rev. Mater.* **2016**, 1, 16013.
- [5] N.-Y. Park, H.-U. Lee, T.-Y. Yu, I.-S. Lee, H. Kim, S.-M. Park, H.-G. Jung, Y.-C. Jung, Y.-K. Sun, *Nat. Energy* **2025**, 10, 479.
- [6] H. Wang, D. Yan, H. Liu, S. Li, X. Niu, C. Ouyang, H. Li, L. Wang, *Adv. Mater.* **2025**, 37, 2509760;.
- [7] C. L. Campion, W. Li, B. L. Lucht, *J. Electrochem. Soc.* **2005**, 152, A2327.
- [8] J. Lopez, D. G. Mackanic, Y. Cui, Z. Bao, *Nat. Rev. Mater.* **2019**, 4, 312.
- [9] D. Zhou, D. Shanmukaraj, A. Tkacheva, M. Armand, G. Wang, *Chem* **2019**, 5, 2326.
- [10] Z. Li, S. Peng, L. Wei, X. Guo, *Adv. Sci. (Weinh)* **2025**, 12, 10481.
- [11] M. A. Cabañero Martínez, N. Boaretto, A. J. Naylor, F. Alcaide, G. D. Salián, F. Palombarini, E. Ayerbe, M. Borrás, M. Casas-Cabanas, *Adv. Energy Mater.* **2022**, 12, 2201264.
- [12] S. Xiao, L. Ren, W. Liu, L. Zhang, Q. Wang, *Energy Storage Mater.* **2023**, 63, 102970.
- [13] J. Huang, C. Li, D. Jiang, J. Gao, L. Cheng, G. Li, H. Luo, Z. L. Xu, D. M. Shin, Y. Wang, Y. Lu, Y. Kim, *Adv. Funct. Mater.* **2024**, 35, 2411171.
- [14] F. Pei, L. Wu, W. Lin, Y. Zhang, Q. Kang, F. Zhang, Y. Shen, Q. Gao, Z. Huang, Y. Huang, *Review of Materials Research* **2025**, 1, 100013.
- [15] X. Zeng, X. Liu, H. Zhu, J. Zhu, J. Lan, Y. Yu, Y. S. Lee, X. Yang, *Adv. Energy Mater.* **2024**, 14, 2402671.
- [16] L.-Z. Fan, H. He, C.-W. Nan, *Nat. Rev. Mater.* **2021**, 6, 1003.
- [17] S. Zou, Y. Yang, J. M. Rupp, B. Yildiz, *Chem. Soc. Rev.* **2025**, 54, 178.
- [18] L. Huang, Y. Wu, P. Luo, K. Su, X. Song, M. Liu, M. Li, H. Song, Z. Cui, *J. Energy Chem.* **2026**, 112, 656.
- [19] X. Y. Huang, C. Z. Zhao, W. J. Kong, N. Yao, Z. Y. Shuang, P. Xu, S. Sun, Y. Lu, W. Z. Huang, J. L. Li, L. Shen, X. Chen, J. Q. Huang, L. A. Archer, Q. Zhang, *Nature* **2025**, 646, 343.
- [20] S. C. Sand, J. L. M. Rupp, B. Yildiz, *Chem. Soc. Rev.* **2025**, 54, 178.
- [21] S. Lv, J. Wang, Y. Zhai, Y. Chen, J. Yang, Z. Zhu, R. Peng, X. Fu, W. Yang, Y. Wang, *Nanomicro Lett* **2025**, 18, 46;.
- [22] F. Elizalde, J. Amici, S. Trano, G. Vozzolo, R. Aguirresarobe, D. Versaci, S. Bodoardo, D. Mecerreyes, H. Sardon, F. Bella, *J. Mater. Chem. A* **2022**, 10, 12588.
- [23] J. Huang, S. Wang, J. Chen, C. Chen, E. Lizundia, *Adv. Mater.* **2025**, 37, 2416733;.
- [24] J. Li, Z. Hu, S. Zhang, H. Zhang, S. Guo, G. Zhong, Y. Qiao, Z. Peng, Y. Li, S. Chen, G. Chen, A.-M. Cao, *Nat. Sustain.* **2024**, 7, 1481.
- [25] J. C. Barbosa, R. Goncalves, C. M. Costa, S. Lanceros-Mendez, *ACS Omega* **2022**, 7, 14457.
- [26] Y. Xiao, Y. Wang, S.-H. Bo, J. C. Kim, L. J. Miara, G. Ceder, *Nat. Rev. Mater.* **2019**, 5, 105.
- [27] Z. Xue, D. He, X. Xie, *J. Mater. Chem. A* **2015**, 3, 19218.
- [28] A. Arya, A. L. Sharma, *Ionics* **2017**, 23, 497.
- [29] S. N. F. Yusuf, S. Z. Yusof, M. Z. Kufian, L. P. Teo, *Materials Today: Proceedings* **2019**, 17, 446.
- [30] K. Nie, Y. Hong, J. Qiu, Q. Li, X. Yu, H. Li, L. Chen, *Front Chem* **2018**, 6, 616.
- [31] Z. Wang, D. Santhanagopalan, W. Zhang, F. Wang, H. L. Xin, K. He, J. Li, N. Dudney, Y. S. Meng, *Nano Lett.* **2016**, 16, 3760.
- [32] G. Xiao, H. Xu, C. Bai, M. Liu, Y. B. He, *Interdisciplinary Materials* **2023**, 2, 609.
- [33] Y. G. Cho, C. Hwang, D. S. Cheong, Y. S. Kim, H. K. Song, *Adv. Mater.* **2019**, 31, 1804909;.
- [34] S. Z. Zhang, X. H. Xia, D. Xie, R. C. Xu, Y. J. Xu, Y. Xia, J. B. Wu, Z. J. Yao, X. L. Wang, J. P. Tu, *J. Power Sources* **2019**, 409, 31.
- [35] Q. Zhao, X. Liu, S. Stalin, K. Khan, L. A. Archer, *Nat. Energy* **2019**, 4, 365.
- [36] V. Vijayakumar, B. Anothumakkool, A. Torris A T, S. B. Nair, M. V. Badiger, S. Kurungot, *J. Mater. Chem. A* **2017**, 5, 8461.
- [37] M. Sun, Z. Zeng, W. Zhong, Z. Han, L. Peng, S. Cheng, J. Xie, *Batteries Supercaps* **2022**, 5, 202200338.
- [38] Q. Ma, S. Fu, A. J. Wu, Q. Deng, W. D. Li, D. Yue, B. Zhang, X. W. Wu, Z. L. Wang, Y. G. Guo, *Adv. Energy Mater.* **2023**, 13, 2203892.
- [39] Q. Liu, L. Wang, X. He, *Adv. Energy Mater.* **2023**, 13, 2300798.
- [40] S. Qin, Y. Yu, J. Zhang, Y. Ren, C. Sun, S. Zhang, L. Zhang, W. Hu, H. Yang, D. Yang, *Adv. Energy Mater.* **2023**, 13, 2301470;.
- [41] I. Shaji, D. Diddens, M. Winter, J. R. Nair, *Energy & Environmental Materials* **2023**, 6, 12469.
- [42] T. Zhu, G. Liu, D. Chen, J. Chen, P. Qi, J. Sun, X. Gu, S. Zhang, *Energy Storage Mater.* **2022**, 50, 495.
- [43] Y. Ma, J. Ma, J. Chai, Z. Liu, G. Ding, G. Xu, H. Liu, B. Chen, X. Zhou, G. Cui, L. Chen, *ACS Appl. Mater. Interfaces* **2017**, 9, 41462;.
- [44] S. Huang, Z. Cui, L. Qiao, G. Xu, J. Zhang, K. Tang, X. Liu, Q. Wang, X. Zhou, B. Zhang, G. Cui, *Electrochim. Acta* **2019**, 299, 820.
- [45] S. J. Yang, N. Yao, F. N. Jiang, J. Xie, S. Y. Sun, X. Chen, H. Yuan, X. B. Cheng, J. Q. Huang, Q. Zhang, *Angew Chem Int Ed Engl* **2022**, 61, 202214545.
- [46] W. Liang, X. Zhou, B. Zhang, Z. Zhao, X. Song, K. Chen, L. Wang, Z. Ma, J. Liu, *Angew Chem Int Ed Engl* **2024**, 63, 202320149;.
- [47] X. Wang, Z. Wang, Z. Li, K. Sun, *Chin. Chem. Lett.* **2023**, 34, 108045.
- [48] Y. Liu, H. Zou, Z. Huang, Q. Wen, J. Lai, Y. Zhang, J. Li, K. Ding, J. Wang, Y.-Q. Lan, Q. Zheng, *Energy Environ. Sci.* **2023**, 16, 6110.
- [49] Y. Liu, Z. Jin, Z. Liu, H. Xu, F. Sun, X. Q. Zhang, T. Chen, C. Wang, *Angew Chem Int Ed Engl* **2024**, 63, 202405802.
- [50] J. Yu, X. Lin, J. Liu, J. T. T. Yu, M. J. Robson, G. Zhou, H. M. Law, H. Wang, B. Z. Tang, F. Ciucci, *Adv. Energy Mater.* **2021**, 12, 2102932;.
- [51] X. Chen, C. Qin, F. Chu, F. Li, J. Liu, F. Wu, *Energy Environ. Sci.* **2025**, 18, 910.
- [52] R. Miao, J. Yang, X. Feng, H. Jia, J. Wang, Y. Nuli, *J. Power Sources* **2014**, 271, 291.
- [53] P. Cheng, H. Zhang, Q. Ma, W. Feng, H. Yu, X. Huang, M. Armand, Z. Zhou, *Electrochim. Acta* **2020**, 363, 137198.
- [54] Y. Chen, Y. Cui, S. Wang, Y. Xiao, J. Niu, J. Huang, F. Wang, S. Chen, *Adv. Mater.* **2023**, 35, 2300982.

- [55] O. Nuyken, S. Pask, *Polymers* **2013**, *5*, 361.
- [56] V. Vijayakumar, B. Anothumakkool, S. Kurungot, M. Winter, J. R. Nair, *Energy Environ. Sci.* **2021**, *14*, 2708.
- [57] G. Moad, E. Rizzardo, in *Nitroxide Mediated Polymerization: From Fundamentals to Applications in Materials Science* (Ed: D. Gigmes) The Royal Society of Chemistry, Piccadilly, London, United Kingdom, **2015**, pp. 3–4.
- [58] J. W. Baker, M. M. Davies, J. Gaunt, *J. Chem. Soc.* **1949**, *0*, 24.
- [59] E. Delebecq, J. P. Pascault, B. Boutevin, F. Ganachaud, *Chem. Rev.* **2013**, *113*, 80.
- [60] F. Pei, Y. Huang, L. Wu, S. Zhou, Q. Kang, W. Lin, Y. Liao, Y. Zhang, K. Huang, Y. Shen, L. Yuan, S. G. Sun, Z. Li, Y. Huang, *Adv. Mater.* **2024**, *36*, 2409269.
- [61] X. Miao, J. Hong, S. Huang, C. Huang, Y. Liu, M. Liu, Q. Zhang, H. Jin, *Adv. Funct. Mater.* **2024**, *35*, 2411751.
- [62] Q. Zhou, J. Ma, S. Dong, X. Li, G. Cui, *Adv. Mater.* **2019**, *31*, 1902029.
- [63] P. Li, J. Hao, S. He, Z. Chang, X. Li, R. Wang, W. Ma, J. Wang, Y. Lu, H. Li, L. Zhang, W. Zhou, *Nat. Commun.* **2025**, *16*, 3727.
- [64] Z. Wang, J. Chen, J. Fu, Z. Li, X. Guo, *Energy Materials* **2024**, *4*.
- [65] C. Xiong, Y. Meng, Y. Wang, B. Ling, M. Ma, H. Yan, F. Kang, D. Zhou, B. Li, *Energy Environ. Sci.* **2025**, *18*, 1612.
- [66] X. Song, R. Zhao, J. Zhu, J. Zhang, N. Xu, J. Liu, Y. Liu, H. Zhang, Y. Ma, C. Li, Y. Chen, *Natl. Sci. Rev.* **2025**, *12*, nwaf016.
- [67] S. Guo, S. Tan, J. Ma, L. Chen, K. Yang, Q. Zhu, Y. Ma, P. Shi, Y. Wei, X. An, Q. Ren, Y. Huang, Y. Zhu, Y. Cheng, W. Lv, T. Hou, M. Liu, Y.-B. He, Q.-H. Yang, F. Kang, *Energy Environ. Sci.* **2024**, *17*, 3797.
- [68] H. Wang, J. Song, K. Zhang, Q. Fang, Y. Zuo, T. Yang, Y. Yang, C. Gao, X. Wang, Q. Pang, D. Xia, *Energy Environ. Sci.* **2022**, *15*, 5149.
- [69] Y. Hu, W. Li, J. Zhu, S.-M. Hao, X. Qin, L.-Z. Fan, L. Zhang, W. Zhou, *Next Energy* **2023**, *1*, 100042.
- [70] L. Ma, J. Tan, Z. Ren, B. Feng, Z. Liu, P. Yi, S. Cao, W. Lu, Y. Liu, C. Ye, M. Ye, H. Fang, J. Shen, *Adv. Funct. Mater.* **2024**, *35*, 2414816.
- [71] W. Zhou, Z. Wang, Y. Pu, Y. Li, S. Xin, X. Li, J. Chen, J. B. Goodenough, *Adv. Mater.* **2019**, *31*, 1805574.
- [72] S. Choudhury, Z. Tu, A. Nijamudheen, M. J. Zachman, S. Stalin, Y. Deng, Q. Zhao, D. Vu, L. F. Kourkoutis, J. L. Mendoza-Cortes, L. A. Archer, *Nat. Commun.* **2019**, *10*, 3091.
- [73] M. Zhang, H. Wang, A. Shao, Z. Wang, X. Tang, S. Li, J. Liu, Y. Ma, *Adv. Energy Mater.* **2024**, *14*, 2303932.
- [74] Z. Song, F. Chen, M. Martinez-Ibanez, W. Feng, M. Forsyth, Z. Zhou, M. Armand, H. Zhang, *Nat. Commun.* **2023**, *14*, 4884.
- [75] C. Zhang, Z. Li, S. Wang, C. Li, Y. Si, Y. Ma, D. Song, H. Zhang, X. Shi, L. Zhang, *Energy Material Advances* **2025**, *6*, 0188.
- [76] P. Shi, J. Ma, M. Liu, S. Guo, Y. Huang, S. Wang, L. Zhang, L. Chen, K. Yang, X. Liu, Y. Li, X. An, D. Zhang, X. Cheng, Q. Li, W. Lv, G. Zhong, Y. B. He, F. Kang, *Nat. Nanotechnol.* **2023**, *18*, 602.
- [77] Y. Ma, L. Chen, Y. Li, B. Li, X. An, X. Cheng, H. Su, K. Yang, G. Xiao, Y. Zhao, Z. Han, S. Guo, J. Mi, P. Shi, M. Liu, Y.-B. He, F. Kang, *Energy Environ. Sci.* **2025**, *18*, 3730.
- [78] Q. Zhu, K. Yang, L. Chen, X. An, S. Guo, Y. Li, Y. Ma, Y. Cao, M. Liu, Y. B. He, *Angew Chem Int Ed Engl* **2025**, *64*, 202425221.
- [79] K. Yang, J. Ma, Y. Li, J. Jiao, S. Jiao, X. An, G. Zhong, L. Chen, Y. Jiang, Y. Liu, D. Zhang, J. Mi, J. Biao, B. Li, X. Cheng, S. Guo, Y. Ma, W. Hu, S. Wu, J. Zheng, M. Liu, Y. B. He, F. Kang, *J. Am. Chem. Soc.* **2024**, *146*, 11371.
- [80] W. Lin, X. Zheng, S. Ma, K. Ji, C. Wang, M. Chen, *ACS Appl. Mater. Interfaces* **2023**, *15*, 8128.
- [81] K.-q. Yu, Z.-s. Li, J. Sun, *Macromol. Theory Simul.* **2001**, *10*, 624.
- [82] M. Gao, D. Zhou, B. Wen, S. Zhu, J. Ni, *Adv. Funct. Mater.* **2025**, *35*, 2500727.
- [83] Y. Ren, S. Chen, M. Odziomek, J. Guo, P. Xu, H. Xie, Z. Tian, M. Antonietti, T. Liu, *Angew Chem Int Ed Engl* **2025**, *64*, 202422169.
- [84] F. Fu, W. Lu, Y. Zheng, K. Chen, C. Sun, L. Cong, Y. Liu, H. Xie, L. Sun, *J. Power Sources* **2021**, *484*, 229186.
- [85] Z. Wei, S. Chen, J. Wang, Z. Wang, Z. Zhang, X. Yao, Y. Deng, X. Xu, *J. Mater. Chem. A* **2018**, *6*, 13438.
- [86] A. J. Butzelaar, P. Roring, T. P. Mach, M. Hoffmann, F. Jeschull, M. Wilhelm, M. Winter, G. Bruncklaus, P. Theato, *ACS Appl. Mater. Interfaces* **2021**, *13*, 39257.
- [87] X. Liu, L. Sun, F. Zhai, T. Wu, P. Wang, H. Du, Y. Xu, X. Wang, *Adv. Energy Mater.* **2025**, *15*, 2405433.
- [88] Y. Shi, N. Yang, J. Niu, S. Yang, F. Wang, *Adv. Sci. (Weinh)* **2022**, *9*, 2200553.
- [89] Y. Zheng, X. Li, C. Y. Li, *Energy Storage Mater.* **2020**, *29*, 42.
- [90] C.-C. Cheng, D.-J. Lee, *RSC Adv.* **2016**, *6*, 38223.
- [91] X. Wu, W. Zhang, H. Qu, C. Guan, C. Li, G. Lu, C. Chang, Z. Lao, Y. Zhu, L. Nie, G. Zhou, *Energy Environ. Sci.* **2025**, *18*, 1835.
- [92] D. Hu, H. Huang, C. Wang, Q. Hong, H. Wang, S. Tang, H. Zhang, J. Li, L. Hu, L. Jiang, X. Fu, J. Lei, Z. Liu, X. He, *Adv. Energy Mater.* **2025**, *15*, 2406176.
- [93] L. Qiao, S. R. Pena, M. Martinez-Ibanez, A. Santiago, I. Aldalur, E. Lobato, E. Sanchez-Diez, Y. Zhang, H. Manzano, H. Zhu, M. Forsyth, M. Armand, J. Carrasco, H. Zhang, *J. Am. Chem. Soc.* **2022**, *144*, 9806.
- [94] Y. Ye, X. Zhu, N. Meng, F. Lian, *Adv. Funct. Mater.* **2023**, *33*, 2307045.
- [95] L. Li, H. Duan, J. Li, L. Zhang, Y. Deng, G. Chen, *Adv. Energy Mater.* **2021**, *11*, 2003154.
- [96] J. Zheng, Y. Y. Hu, *ACS Appl. Mater. Interfaces* **2018**, *10*, 4113.
- [97] J. Xiao, *Science* **2019**, *366*, 426.
- [98] Y. Liu, D. Lin, Y. Jin, K. Liu, X. Tao, Q. Zhang, X. Zhang, Y. Cui, *Sci. Adv.* **2017**, *3*, aao0713.
- [99] X. Yang, X. Gao, S. Mukherjee, K. Doyle-Davis, J. Fu, W. Li, Q. Sun, F. Zhao, M. Jiang, Y. Hu, H. Huang, L. Zhang, S. Lu, R. Li, T. K. Sham, C. V. Singh, X. Sun, *Adv. Energy Mater.* **2020**, *10*, 2001191.
- [100] X. Wang, Z. Chen, W. Wang, R. Zhan, Y. Sun, *Adv. Funct. Mater.* **2025**, *35*, 2500288.
- [101] D. T. Boyle, Y. Li, A. Pei, R. A. Vila, Z. Zhang, P. Sayavong, M. S. Kim, W. Huang, H. Wang, Y. Liu, R. Xu, R. Sinclair, J. Qin, Z. Bao, Y. Cui, *Nano Lett.* **2022**, *22*, 8224.
- [102] L. Xu, X. Xiao, H. Tu, F. Zhu, J. Wang, H. Liu, W. Huang, W. Deng, H. Hou, T. Liu, X. Ji, K. Amine, G. Zou, *Adv. Mater.* **2023**, *35*, 2303193.
- [103] M. Cui, N. Gao, W. Zhao, H. Zhao, Z. Cao, Y. Qin, G. Gao, K. Xi, Y. Su, S. Ding, *Adv. Energy Mater.* **2024**, *14*, 2303834.
- [104] T. Zhou, Y. Zhao, J. W. Choi, A. Coskun, *Angew Chem Int Ed Engl* **2021**, *60*, 22791.
- [105] Y. He, C. Wang, P. Zou, R. Lin, E. Hu, H. L. Xin, *Angew Chem Int Ed Engl* **2023**, *62*, 202308309.
- [106] K. Liu, A. Pei, H. R. Lee, B. Kong, N. Liu, D. Lin, Y. Liu, C. Liu, P. C. Hsu, Z. Bao, Y. Cui, *J. Am. Chem. Soc.* **2017**, *139*, 4815.
- [107] Z. Huang, H. Lyu, L. C. Greenburg, Y. Cui, Z. Bao, *Nat. Energy* **2025**, *10*, 811.
- [108] G. Zheng, C. Wang, A. Pei, J. Lopez, F. Shi, Z. Chen, A. D. Sendek, H.-W. Lee, Z. Lu, H. Schneider, M. M. Safont-Sempere, S. Chu, Z. Bao, Y. Cui, *ACS Energy Lett.* **2016**, *1*, 1247.
- [109] C. Zhu, T. Fuchs, S. A. L. Weber, F. H. Richter, G. Glasser, F. Weber, H. J. Butt, J. Janek, R. Berger, *Nat. Commun.* **2023**, *14*, 1300.
- [110] W. Zhang, V. Koverga, S. Liu, J. Zhou, J. Wang, P. Bai, S. Tan, N. K. Dandu, Z. Wang, F. Chen, J. Xia, H. Wan, X. Zhang, H. Yang, B. L. Lucht, A.-M. Li, X.-Q. Yang, E. Hu, S. R. Raghavan, A. T. Ngo, C. Wang, *Nat. Energy* **2024**, *9*, 386.
- [111] Y. Yang, L. G. Yu, Y. X. Huang, X. Q. Ding, Z. Q. Xue, Z. Li, Y. X. Yao, S. Zhang, L. Xu, X. F. Wen, J. Pei, C. Yan, J. Q. Huang, *Angew Chem Int Ed Engl* **2025**, *64*, 202503616.
- [112] H. Chen, M. Zheng, S. Qian, H. Y. Ling, Z. Wu, X. Liu, C. Yan, S. Zhang, *Carbon Energy* **2021**, *3*, 929.
- [113] S. Zhang, B. Xie, X. Zhuang, S. Wang, L. Qiao, S. Dong, J. Ma, Q. Zhou, H. Zhang, J. Zhang, J. Ju, G. Xu, Z. Cui, G. Cui, *Adv. Funct. Mater.* **2023**, *34*, 2314063.

- [114] J. Guo, X. Liu, Z. Shen, Y. Lv, X. Zhang, C. Zhang, X. Zhang, *Adv. Funct. Mater.* **2024**, *34*, 2405951.
- [115] C. Fu, X. Zhang, H. Huo, J. Zhu, H. Xu, L. Wang, Y. Ma, Y. Gao, G. Yin, P. Zuo, J. Lu, *Adv. Funct. Mater.* **2023**, *34*, 2312187.
- [116] K. Ma, Y. Cao, S. Zhang, Y. Zhang, S. Fang, X. Han, F. Jin, J. Sun, *Nano Lett.* **2024**, *24*, 8826.
- [117] J. K. Hu, Y. C. Gao, S. J. Yang, X. L. Wang, X. Chen, Y. L. Liao, S. Li, J. Liu, H. Yuan, J. Q. Huang, *Adv. Funct. Mater.* **2024**, *34*, 2311633.
- [118] K. Su, P. Luo, Y. Wu, X. Song, L. Huang, S. Zhang, H. Song, L. Du, Z. Cui, *Adv. Funct. Mater.* **2024**, *34*, 2409492.
- [119] A. Santiago, J. Castillo, I. Garbayo, A. Saenz de Buruaga, J. A. Coca Clemente, L. Qiao, R. Cid Barreno, M. Martinez-Ibañez, M. Armand, H. Zhang, C. Li, *ACS Appl. Energy Mater.* **2021**, *4*, 4459.
- [120] S. Kim, S. O. Park, M.-Y. Lee, J.-A. Lee, I. Kristanto, T. K. Lee, D. Hwang, J. Kim, T.-U. Wi, H.-W. Lee, S. K. Kwak, N.-S. Choi, *Energy Storage Mater.* **2022**, *45*, 1.
- [121] Y. Li, F. Bai, C. Li, Y. Wang, T. Li, *Adv. Energy Mater.* **2024**, *14*, 2304414.
- [122] D. Zhang, Y. Liu, D. Li, S. Li, Q. Xiong, Z. Huang, S. Wang, H. Hong, J. Zhu, H. Lv, C. Zhi, *Energy Environ. Sci.* **2025**, *18*, 227.
- [123] Y. Zhao, T. Zhou, M. Mensi, J. W. Choi, A. Coskun, *Nat. Commun.* **2023**, *14*, 299.
- [124] S. Zhang, Z. Li, Y. Zhang, X. Wang, P. Dong, S. Lei, W. Zeng, J. Wang, X. Liao, X. Chen, D. Li, S. Mu, *Energy Environ. Sci.* **2025**, *18*, 3807.
- [125] G. Ye, X. Hong, M. He, J. Song, L. Zhu, C. Zheng, Y. Ma, Y. An, K. Shen, W. Shi, Y. Jia, M. B. Shafiqat, P. Gao, D. Xia, F. Chen, Q. Pang, *Adv. Mater.* **2025**, *37*, 2417829.
- [126] L. Chen, T. Gu, J. Ma, K. Yang, P. Shi, J. Biao, J. Mi, M. Liu, W. Lv, Y.-B. He, *Nano Energy* **2022**, *100*, 107470.
- [127] Q. Liu, G. Yang, X. Li, S. Zhang, R. Chen, X. Wang, Y. Gao, Z. Wang, L. Chen, *Energy Storage Mater.* **2022**, *51*, 443.
- [128] Y. Zhu, Z. Lao, M. Zhang, T. Hou, X. Xiao, Z. Piao, G. Lu, Z. Han, R. Gao, L. Nie, X. Wu, Y. Song, C. Ji, J. Wang, G. Zhou, *Nat. Commun.* **2024**, *15*, 3914.
- [129] M. Balaish, J. C. Gonzalez-Rosillo, K. J. Kim, Y. Zhu, Z. D. Hood, J. L. M. Rupp, *Nat. Energy* **2021**, *6*, 227.
- [130] Y. Liang, S. Guan, C. Xin, K. Wen, C. Xue, H. Chen, S. Liu, X. Wu, H. Yuan, L. Li, C. W. Nan, *ACS Appl. Mater. Interfaces* **2022**, *14*, 32075.
- [131] W. Bao, Y. Zhang, L. Cao, Y. Jiang, H. Zhang, N. Zhang, Y. Liu, P. Yan, X. Wang, Y. Liu, H. Li, Y. Zhao, J. Xie, *Adv. Mater.* **2023**, *35*, 2304712.
- [132] Y. Fu, Z. Gu, Q. Gan, Y.-W. Mai, *Materials Science and Engineering: R: Reports* **2024**, *160*, 100815.
- [133] Y. Ma, C. Wang, K. Yang, B. Li, Y. Li, S. Guo, J. Lv, X. An, M. Liu, Y. B. He, F. Kang, *ACS Appl. Mater. Interfaces* **2023**, *15*, 17978.
- [134] H. Peng, T. Long, J. Peng, H. Chen, L. Ji, H. Sun, L. Huang, S. G. Sun, *Adv. Energy Mater.* **2024**, *14*, 2400428.
- [135] F. Fu, Y. Zheng, N. Jiang, Y. Liu, C. Sun, A. Zhang, H. Teng, L. Sun, H. Xie, *Chem. Eng. J.* **2022**, *450*, 137776.
- [136] H. He, N. Deng, X. Wang, L. Gao, C. Tang, E. Wu, J. Ren, X. Yang, N. Feng, D. Gao, X. Zhuang, *Adv. Funct. Mater.* **2025**, *35*, 2421670.
- [137] A. H. Ban, S.-J. Pyo, W. J. Bae, H.-S. Woo, J. Moon, D.-W. Kim, *Chem. Eng. J.* **2023**, *475*, 146266.
- [138] M. Yao, Q. Ruan, T. Yu, H. Zhang, S. Zhang, *Energy Storage Mater.* **2022**, *44*, 93.
- [139] Y. Zhou, L. Wei, X. Guo, *EnergyChem* **2025**, *7*, 100154.
- [140] X. Yi, Y. Yang, K. Xiao, S. Zhang, B. Wang, N. Wu, B. Cao, K. Zhou, X. Zhao, K. W. Leong, X. Wang, W. Pan, H. Li, *Adv. Energy Mater.* **2025**, *15*, 2404973.
- [141] M. Liu, P. Chen, X. Pan, S. Pan, X. Zhang, Y. Zhou, M. Bi, J. Sun, S. Yang, A. L. Vasiliev, P. J. Kulesza, X. Ouyang, J. Xu, X. Wang, J. Zhu, Y. Fu, *Adv. Funct. Mater.* **2022**, *32*, 2205031.
- [142] L. Zhao, Y. Du, E. Zhao, C. Li, Z. Sun, Y. Li, H. Li, *Adv. Funct. Mater.* **2023**, *33*, 2214881.
- [143] T. Munaoka, X. Yan, J. Lopez, J. W. F. To, J. Park, J. B. H. Tok, Y. Cui, Z. Bao, *Adv. Energy Mater.* **2018**, *8*, 1703138.
- [144] B. Zhou, Y. H. Jo, R. Wang, D. He, X. Zhou, X. Xie, Z. Xue, *J. Mater. Chem. A* **2019**, *7*, 10354.
- [145] C. H. Li, C. Wang, C. Keplinger, J. L. Zuo, L. Jin, Y. Sun, P. Zheng, Y. Cao, F. Lissel, C. Linder, X. Z. You, Z. Bao, *Nat. Chem.* **2016**, *8*, 618.
- [146] J. F. Mei, X. Y. Jia, J. C. Lai, Y. Sun, C. H. Li, J. H. Wu, Y. Cao, X. Z. You, Z. Bao, *Macromol. Rapid Commun.* **2016**, *37*, 1667.
- [147] Y. He, C. Wang, R. Zhang, P. Zou, Z. Chen, S. M. Bak, S. E. Trask, Y. Du, R. Lin, E. Hu, H. L. Xin, *Nat. Commun.* **2024**, *15*, 10015.
- [148] H. Guo, Y. Han, W. Zhao, J. Yang, L. Zhang, *Nat. Commun.* **2020**, *11*, 2037.
- [149] B. Zhou, T. Deng, C. Yang, M. Wang, H. Yan, Z. Yang, Z. Wang, Z. Xue, *Adv. Funct. Mater.* **2023**, *33*, 2212005.
- [150] P. H. Duan, J. L. Yu, Q. S. Liu, G. Wu, X. L. Wang, Y. Z. Wang, *Adv. Funct. Mater.* **2024**, *34*, 2402065.
- [151] S. Lee, J. Song, J. Cho, J. G. Son, T. A. Kim, *ACS Appl. Polym. Mater.* **2023**, *5*, 7433.
- [152] D. Liu, Z. Tang, L. Luo, W. Yang, Y. Liu, Z. Shen, X. H. Fan, *ACS Appl. Mater. Interfaces* **2021**, *13*, 36320.
- [153] F. Pei, L. Wu, Y. Zhang, Y. Liao, Q. Kang, Y. Han, H. Zhang, Y. Shen, H. Xu, Z. Li, Y. Huang, *Nat. Commun.* **2024**, *15*, 351.
- [154] S.-J. Tan, J. Yue, Z. Chen, X.-X. Feng, J. Zhang, Y.-X. Yin, L. Zhang, J.-C. Zheng, Y. Luo, S. Xin, Y.-G. Guo, *Energy Material Advances* **2024**, *5*, 0076.
- [155] Y. Cui, J. Wan, Y. Ye, K. Liu, L. Y. Chou, Y. Cui, A. Fireproof, *Nano Lett.* **2020**, *20*, 1686.
- [156] L. Han, L. Wang, Z. Chen, Y. Kan, Y. Hu, H. Zhang, X. He, *Adv. Funct. Mater.* **2023**, *33*, 2300892.
- [157] Q. Zhang, T. Bian, X. Wang, R. Shi, Y. Zhao, *Angew Chem Int Ed Engl* **2025**, *64*, 202415343.
- [158] W. Tang, T. Zhou, Y. Duan, M. Zhou, Z. Li, R. Liu, *Carbon Neutralization* **2024**, *3*, 386.
- [159] H. An, M. Li, Q. Liu, Y. Song, J. Liu, Z. Yu, X. Liu, B. Deng, J. Wang, *Nat. Commun.* **2024**, *15*, 9150.
- [160] N. Xu, Y. Zhao, M. Ni, J. Zhu, X. Song, X. Bi, J. Zhang, H. Zhang, Y. Ma, C. Li, Y. Chen, *Angew Chem Int Ed Engl* **2024**, *63*, 202404400.
- [161] K. Chen, A. Hu, W. Yang, Y. Li, Z. W. Seh, F. Li, J. Long, S. Chen, *Adv. Funct. Mater.* **2025**, *13*, 13143.
- [162] M. Ding, Y. Peng, J. Tong, X. Feng, Y. Xing, L. Wang, X. Wu, S. Zhang, M. Ouyang, *Small* **2025**, *21*, 2410961.
- [163] A. Perea, M. Dontigny, K. Zaghbi, *J. Power Sources* **2017**, *359*, 182.
- [164] B. S. Vishnugopi, M. T. Hasan, H. Zhou, P. P. Mukherjee, *ACS Energy Lett.* **2022**, *8*, 398.
- [165] L. Chen, T. Gu, J. Mi, Y. Li, K. Yang, J. Ma, X. An, Y. Jiang, D. Zhang, X. Cheng, S. Guo, Z. Han, T. Hou, Y. Cao, M. Liu, W. Lv, Y. B. He, F. Kang, *Nat. Commun.* **2025**, *16*, 3517.
- [166] J. Zhu, P. Bian, G. Sun, J. Zhang, G. Lou, X. Song, R. Zhao, J. Liu, N. Xu, A. Li, X. Wan, Y. Ma, C. Li, H. Zhang, Y. Chen, *Angew Chem Int Ed Engl* **2025**, *64*, 202424685.
- [167] T. Hou, D. Wang, B. Jiang, Y. Liu, J. Kong, Y. He, Y. Huang, H. Xu, *Nat. Commun.* **2025**, *16*, 962.
- [168] S. Liu, W. Tian, J. Shen, Z. Wang, H. Pan, X. Kuang, C. Yang, S. Chen, X. Han, H. Quan, S. Zhu, *Nat. Commun.* **2025**, *16*, 2474.
- [169] W. Xu, A. Hu, R. Zheng, Y. Li, K. Chen, J. Chen, Z. Wang, R. Xu, J. Wang, F. Li, J. Long, F. Wu, *Adv. Funct. Mater.* **2025**, *11*, 1135.
- [170] Q. Yu, Y. Liang, X. Wu, X. Zhang, H. Lu, M. Li, J. Yao, Z. Rong, Z. Yu, S. Gu, B. Zhang, Y. Tang, J. Huang, *Energy Storage Mater.* **2025**, *80*, 104383.
- [171] B. Yang, Y. Pan, T. Li, A. Hu, K. Li, B. Li, L. Yang, J. Long, *Energy Storage Mater.* **2024**, *65*, 103124.
- [172] X. Zhou, Y. Chen, F. Zhen, Y. Wu, W. Li, X. Yin, L. Liu, S. Ding, W. Yu, *ACS Nano* **2025**, *19*, 14073.
- [173] J. Zhu, R. Zhao, J. Zhang, X. Song, J. Liu, N. Xu, H. Zhang, X. Wan, X. Ji, Y. Ma, C. Li, Y. Chen, *Angew Chem Int Ed Engl* **2024**, *63*, 202400303.

- [174] S. Li, H. Hong, X. Yang, D. Li, Q. Xiong, D. Zhang, S. Wang, Z. Huang, H. Lv, C. Zhi, *Adv. Mater.* **2025**, *37*, 2504333.
- [175] H. Wang, J. Yang, X. Xu, J. Geng, X. Lin, H. Xu, Y. Huang, *Adv. Mater.* **2025**, *37*, 04625.
- [176] H. Huo, K. Huang, W. Luo, J. Meng, L. Zhou, Z. Deng, J. Wen, Y. Dai, Z. Huang, Y. Shen, X. Guo, X. Ji, Y. Huang, *ACS Energy Lett.* **2022**, *7*, 650.
- [177] K. Zhao, X. Wan, Y. Lin, H. Wu, X. Tan, S. Zou, M. Zhu, J. Liu, *Adv. Energy Mater.* **2024**, *15*, 2404295.
- [178] O. T. Unke, S. Chmiela, H. E. Saucedo, M. Gastegger, I. Poltavsky, K. T. Schütt, A. Tkatchenko, K.-R. Müller, *Chem. Rev.* **2021**, *121*, 10142.
- [179] J. Wang, H. Hu, S. Duan, Q. Xiao, J. Zhang, H. Liu, Q. Kang, L. Jia, J. Yang, W. Xu, H. Fei, S. Cheng, L. Li, M. Liu, H. Lin, Y. Zhang, *Adv. Funct. Mater.* **2021**, *32*, 2110468.
- [180] Z. Cheng, H. Lin, Y. Liu, Q. Yan, B. L. Su, H. Zhang, *Adv. Funct. Mater.* **2025**, 2505207.
- [181] K. A. Severson, P. M. Attia, N. Jin, N. Perkins, B. Jiang, Z. Yang, M. H. Chen, M. Aykol, P. K. Herring, D. Fraggedakis, M. Z. Bazant, S. J. Harris, W. C. Chueh, R. D. Braatz, *Nat. Energy* **2019**, *4*, 383.
- [182] Z. Jin, X. Li, Z. Qiu, F. Li, E. Kong, B. Li, *Energy* **2025**, *314*, 134229.



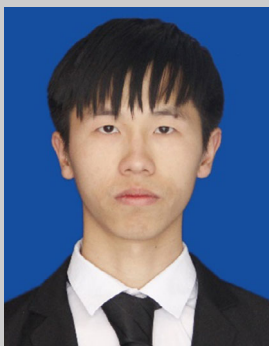
Minkang Jiang is currently studying for a master's degree under the name of Professor Liping Wang of University of Electronic Science and Technology of China. His current research direction is all solid-state lithium battery.



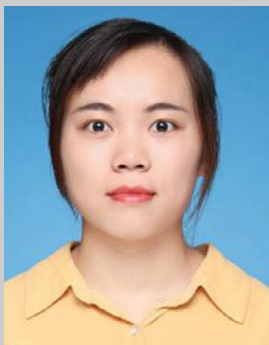
Yuhao Ma is currently pursuing his master's degree under the supervision of Prof. Liping Wang at University of Electronic Science and Technology of China. His research interests focus on high energy density lithium batteries.



Chuang Bao is currently studying for a master's degree under the guidance of Professor Liping Wang at the University of Electronic Science and Technology of China, focusing on high-voltage lithium metal batteries.



Hao Wang is pursuing his doctoral studies at the School of Materials and Energy, University of Electronic Science and Technology of China. His doctoral research centers on the design of electrolytes for high-voltage lithium metal batteries.



Fengrui Zhang received her Ph.D. degree in Physical Chemistry from the University of Science and Technology of China (USTC) in 2022. Then, she served as a Postdoctoral Researcher at the Institute of Physics, Chinese Academy of Sciences from 2023 to 2025, under the supervision of Researcher Li Hong. Currently, she is the Technical Director at Tianmu Lake Advanced Energy Storage Technology Research Institute Co., Ltd. Her research interests focus on the development of key materials and technologies for solid-state lithium batteries, particularly specializing in oxide-polymer composite solid electrolytes and battery technology development.



Heng Zhang received his Ph.D. degree in Chemistry from HUST. Then, he joined CIC EnergiGUNE as a Post Doc Researcher (2016/2017) working with Prof. Michel Armand, and later he acted as the Research Line Manager of Polymer Electrolyte at CIC EnergiGUNE (January 2018/June 2020). Currently, he is a Full Professor of Organic Chemistry at HUST since August 2020. His research interests focus on non-aqueous electrolyte materials, particularly salt anions and solid polymer electrolytes, for rechargeable batteries.



Liping Wang is now a professor at University of Electronic Science and Technology of China. She received her PhD degree (2011) from Institute of Physics, Chinese Academy of Sciences and Laboratoire de réactivité et chimie des solides (LRCS), Université de Picardie Jules Verne, France. She worked as a post-doctoral fellow in Max Planck Institute of Colloids and Interfaces, Germany (2012) and Research Associate at Brookhaven National Lab, United States (2013/2014). Her current research interests are Li-based high energy rechargeable batteries.